Dynamic Responses of Semi-Submersible: A Comparison of Long-Crested and Short-Crested Waves with Current

by

Ng Sok Jin

14776

Dissertation submitted in partial fulfilment of

the requirements for the

Bachelor of Engineering (Hons)

(Civil)

FYP II January 2015

Universiti Teknologi PETRONAS

Bandar Seri Iskandar

31750 Tronoh

Perak Darul Ridzuan

CERTIFICATION OF APPROVAL

Dynamic Responses of Semi-Submersible: A Comparison of Long-Crested and Short-Crested Waves with Current

by

Ng Sok Jin

14776

A project dissertation submitted to the

Civil Engineering Programme

Universiti Teknologi PETRONAS

in partial fulfilment of the requirement for the

BACHELOR OF ENGINEERING (Hons)

(CIVIL)

Approved by,

_____

(Dr. Ng Cheng Yee)

UNIVERSITI TEKNOLOGI PETRONAS

TRONOH, PERAK

January 2015

CERTIFICATION OF ORIGINALITY

This is to certify that I am responsible for the work submitted in this project, that the original work is my own except as specified in the references and acknowledgements, and that the original work contained herein have not been undertaken or done by unspecified sources or persons.

Ng Sok Jin

(NG SOK JIN)

ABSTRACT

As the development of oil and gas industry has progressed into deep-water, the study on deep-water offshore structures has become more important. Among the environmental force acting on the structures, wave forces are the most significant. Waves can be categorized as short-crested waves and long-crested waves based on the direction of propagation. Long-crested waves can be defined as two-dimensional waves, which extend infinitely in lateral direction. On the other hand, short-crested waves consist of a series of long-crested waves with random magnitude and directions in three-dimensional. It is more common to find short-crested waves in the real sea state instead of long-crested waves. Furthermore, no research has been performed on semi-submersible particularly focusing on short-crested waves and current concurrently. Therefore, the study to determine the dynamic responses of one of the deep-water offshore structures, i.e. semi-submersible platforms subjected to short-crested waves and current is more significant. In this study, a numerical comparative study on a typical eight-column semi-submersible model subjected to long-crested and short-crested waves with current had been conducted. In the research, frequency domain method, which adopted the Morison Equation and wave energy spectrum was utilized to obtain the responses in three degrees of freedom i.e. surge, heave, and pitch motion in term of Response Amplitude Operator (RAO). Besides, the maximum amplitude of each motion response was determined and compared. The results indicated that the dynamic responses for short-crested waves are approximately 50% lower than long-crested waves and the effect of current induced is insignificant.

ACKNOWLEDGEMENTS

In the first place, the author of this paper would like to especially deliver her utmost recognition to her direct supervisor-in-charge, Dr. Ng Cheng Yee for her endless support, guidance, advices, and lessons that had been offered throughout her Final Year Project period. Her patient yet passionate supervision assisted the author to overcome various difficulties and problem. Heartfelt appreciation is given sincerely from the author to Dr. Ng who is very pleasing in giving out informational and educational approach. Thank you very much.

In addition, the author would like express her sincere gratitude to Universiti Teknologi PETRONAS (UTP) for offering this beneficial course. It allows substantial learning of valuable knowledge and mentorship system where the author was guided. It also encourages and cultivates problem-solving skills. Last but not least, the author would like to earnestly extend her whole-hearted thanks to Civil Engineering Department for their full assistance and responsive assistance.

TABLE OF CONTENTS

LIST OF FIGURES

LIST OF TABLES

ABBREVIATIONS AND NOMENCLATURES

Abbreviations	Full Naming
F_x	Surge
F_z	Heave
LCW	Long-Crested Waves
M_y	Pitch
RAO	Response Amplitude Operator
SCW	Short-Crested Waves
S(f)	Wave Spectrum
$S_x(f)$	Response Spectrum

CHAPTER 1

INTRODUCTION

1.1 Background

Offshore structures developed rapidly over the last three to four decade in order to increase the oil and gas production. In the year of 1909, the very first discovery of oil in Sarawak state had offered a firm bedrock for the growth of Malaysia's present day oil and gas industry. The 25th largest oil reserves and 14th largest gas reserves in the globe is possessed by Malaysia with latest daily crude production rate of 600 thousand barrels [1]. In view of this, offshore structures inevitably carry significant role and responsibility to extract, process and temporary store crude oil and natural gas until the products can be transported to shore for supplementary refining and marketing.

In Malaysia, there is a wide variety of offshore structures, which can be categorized into either fixed or floating structures in fundamental. For instances, fixed structures in offshore can be steel jacket platform, concrete gravity-based structure, jack-up, and compliant tower. Floating structures consist of semi-submersible, spar, tension leg platform (TLP), and floating, production, storage and offloading (FPSO). Fixed offshore structures are basically constructed by concrete and/or steel, which anchored directly onto the seabed, supporting a topside for drilling, production, and living quarter purposes. Generally, these type of structures are more cost-effective to be built in shallow water up to 520 m depth and steel jacket platform is the most general offshore installation used in Malaysia. The jacket platform was formed as a support system for topside deck, conductors, drilling rigs, risers, facilities, and other appurtenances.

The substructure that made up from reinforced concrete also employed in some offshore structures. This type of fixed offshore structure is known as concrete gravity-based

structure. It mainly depends on its massive self-weight to withstand and resist the lateral environmental loads in offshore region. The reinforced concrete substructure principally comprises of a cellular base surrounding a number of unbraced columns that extend upward and rest on the seabed to support the above water superstructure. It can be built in moderate water depth up to 300 m and its main advantage is cheap maintenance cost.

Kikeh was the first deep-water development in Malaysia, which located in approximately 1350 m water depth. The field situated at 120 km northwest of the island of Labuan, offshore Sabah, East Malaysia and includes of a FPSO vessel for production collected from wells drilled. Kikeh was designed as a truss spar. The structure was held in place by mooring lines whereby it is allowed to move by adjusting the tension of the mooring lines.

Semi-submersible platform, another type of floating offshore platform, has the primary characteristic to float at a stationary location. Also maintain good stability when they encounter the natural environmental forces, but less affected by those loadings than a normal ship due to its hull structure. The structure is made up of topside and hull that provide sufficient buoyancy for floating and sufficient weight to keep the structure upright, where the hull comprises of columns and pontoon. The semi-submersible platforms has better mobility and can be ballasted up or down by changing the amount of water in the buoyancy tanks. The platform usually held in place by anchors connected to the seabed by mooring system, which made up of a combination of chain, wire rope and/or polyester rope. Its location also can be determined by using dynamic positioning system. Particularly, semi-submersibles have advanced capabilities in offshore ultra-deep-water drilling operations with water depth ranging from 600 m to 3600 m. One example of semi-submersible is the Gumusut-Kakap field in Malaysia, which is in water up to 1200 m deep. The platform is developed by using 19 subsea wells with oil exported via a pipeline to the Sabah Oil and Gas Terminal [2].

1.2 Problem Statement

The study of dynamic responses based on short-crested waves is very significant compared to long-crested waves, whereby short-crested waves offer higher accuracy for the simulation of real sea waves. In reality, short-crested waves own the similarity with real waves, which is multi-directional 3D and complex. Thus the use of short-crested wave generation to model the real sea state is the best methodology for design or analysis of the offshore structures. The level of accuracy and percentage of reliability for the results obtained will be relatively higher compared to the study which considers long-crested waves.

Even though the study on short-crested wave is no longer rare in wave simulation effort in this day and age, the research to highlight the dynamic responses of semi-submersible incorporated both short-crested waves and current induced is still not available. Until present, the scope research done has been mainly dedicated on the vertical circular cylinder, wave kinematics, directional wave force, and directional wave spectrum. Therefore, studies on the dynamic responses of semi-submersible affected by the environmental factor of short-crested waves and current is very crucial to be conducted for the sake of knowledge.

Furthermore, it has been highlighted in the research published that the responses due to short-crested waves for surge, heave, and pitch will be lower compared to long-crested waves. If this fact is very well established and proved, it can lead to more economical design of offshore platforms, which will be more favorable in offshore engineering in specific for deep-water challenges. Thus, the motion responses for deep-water offshore structures, when exposed to short-crested wave, will be a very crucial reference in the future.

1.3 Objectives

This study entitled "Dynamic Responses of Semi-Submersible: A Comparison of Long-Crested and Short-Crested Waves with Current" is aimed to achieve the objectives mentioned below. These objectives are generated from an intention to solve the advanced problem statement.

(a) To determine the dynamic reaction of semi-submersible structures subjected to long-crested and short-crested waves with current induced through computing the response amplitude operator (RAO) by using numerical analysis.
(b) To quantify the effectiveness of short-crested waves as compared long-crested waves in the effort of designing offshore structures and optimizing design cost through numerical comparative study.

1.4 Scope of Study

In association with the above objectives, the scope for this study is mainly highlighted the following aspects:

(a) Dynamic reaction of semi-submersible in three degrees of freedom, i.e. the surge, heave, and pitch motion subjected to long-crested waves, short-crested waves, and current
(b) Numerical comparative study by using frequency domain method and wave energy spectrum theories
(c) Response Amplitude Operator (RAO) to evaluate the effectiveness of short-crested waves in optimization of offshore structures design cost

1.5 Relevancy and Feasibility of Study

The relevancy and feasibility of the study have been fulfilled in this project. This project is feasible within the scope of study and time frame for Final Year Project purpose for a Civil Engineering student. It applies a lot of theories and concepts related to offshore structures and deep-water technology subjects, which have been learnt in Civil Engineering Offshore Oil and Gas Structures major courses. Furthermore, it gives deep understanding and knowledge on the real offshore field challenges, which encounter with waves and current these two major environmental forces. Besides, the scope of study was completed within the time frame allocated and achieving the initial goal of Final Year Project.

CHAPTER 2

LITERATURE REVIEW

For the past decades, oil and gas industry has moved towards offshore due to depletion of these energy resources in onshore region. Malaysia is having seven sedimentary basins in deep waters with a huge amount of natural resources. Thus, the knowledge regarding deep-water offshore structures is essential in offshore engineering for planning, design, and construction purposes. In Malaysia, deep-water region was defined as the region where water depth that ranged from 200 meter to 1200 meter, beyond 1200 meter is considered as ultra-deep-water.

The major environmental forces in offshore region consist of waves, current, and wind that acting on the oil and gas exploration structures are of great concern especially in deep-water depth. Among all the environmental forces, waves can be perceived as the most dominant factor governing the structural dynamic responses. In view of the variation and importance of environmental condition, it brings a fact of interest to explore the wave behaviors.

The semi-submersible platform, is one of the widely used platform in deep-water and also ultra-deep-water region for drilling and production purposes. In addition, semi-submersible is a weight-sensitive floating offshore structure that supporting the topside by the mean of multi-legged seated on the full submerged horizontal pontoons. Thus, wave loadings effect on the dynamic motion of semi-submersible is an important research topic to be investigated.

In the past, studies on the wave forces have been conducted intensively by considering waves in two-dimensional, which is commonly termed as long-crested waves. Sun [3] presented a study focused on regular wave forces including the viscous damping effect and viscous exciting effect subjected to semi-submersible. Maeda et al. [4] justified the estimation method of time series responses on floating structure by comparing analytical and measured results. Zhang and Li [5] also computed the wave forces on floating platforms i.e. semi-submersible by using Morison's Equation due to internal solitary long-crested waves. Yilmaz and Incecik [6] established a non-linear time domain analysis to investigate the responses of moored semi-submersible due to waves, wind, and current factors.

In addition, relevant experiment was also carried out by Agarwal and Jain [7] regarding the dynamic response of spar under the influence of unidirectional waves, where spar is another important floating offshore platform used in deep-water drilling activity. In the research, they performed a time domain analysis considering the Newmark's Beta concept. The results of this study was adopted as a good reference for further study on this topic where they concluded that the structure owns higher flexibility and lesser dynamic behavior under the circumstance of lower horizontal forces exerted.

However, the properties and behavior of real wind-generated waves were not accounted in those studies. Thus, short-crested waves were simulated in the following research to represent the real sea state. Ralls and Wiegel [8] simulated short-crested waves by using wind-wave tunnel and they presented three methods to achieve quantitative statistics on short-crested wave pattern, which are the characteristic angle, grid approximation and line-intersection distribution. It was suggested that Fuchs's short-crested wave theory should be taken into account in wave motion study.

Next, both research of Sun [9] and Ji et al. [10] were carried out statistically and experimentally on the relationship between random waves on a huge cylinder in viewing the shortage of validated details in that aspect. From the studies, both of them claimed that directional spreading parameter is the most significant factor influences on circular cylinder when encountering multidirectional waves. It was defined that the broader the directional spreading, the narrower the waves produced. On the other hand, Li and Lin

[11] also considered the interaction between regular and irregular waves affected on floating structures through simulation and experiment.

One of the most significant studies in this aspect was the study regarding diffraction of short-crested waves on a vertical circular cylinder conducted by Zhu [12]. He drawn a conclusion that the force applied on the cylinder is lower in the wave direction than plane incident waves. This study was then further extended by Jian et al. [13] through incorporating current factor. They presented that the cylinder undertakes larger loads when both short-crested waves and current are applied instead of only wave forces. Thus, they recommended that current factor should be considered in marine construction.

Koterayama and Nakamura [14] also measured the three-dimensional wave forces concurrently on vertical cylinder and orbital velocity of waves on a platform. The finding indicates that three-dimensional wave forces could be simplified into two-dimensional and computed by using Morison Equation. Morison's Equation is one of the crucial formulae to be utilized in the research of wave kinematics. In the research paper written by Boccotti et al. [15], both measured and calculated wave loading from Morison's Equation were assessed repeatedly for plenty of trials in laboratory to investigate the effectiveness of the equation. However, this study only focused the effect of wave loading exerted on vertical cylinder. Later on, they deepened the study [16] and concluded that the condition of irregular wind waves applied on vertical and also horizontal cylinder can be simulated effectively with the combination of Morison's Equation and directional wave spectrum. The conclusion was validated through experiment on trimmed vertical cylinder and flooded horizontal cylinder to evaluate the accuracy of the equation.

IAHR working group [17] compared the analysis methods of multidirectional wave basin data with respect to the mean and distribution of wave direction, wave energy dispersal, and reflection coefficients. Several sets of multidirectional waves were subjected to different experimental wave basins by using same incident wave height, direction, and period. From their studies, they found that it is not consistent between the results from various methods and the selection of method between high or low resolution depends on the wave field. Based on the research conducted by Fenton [18], the accuracy of various wave analysis approaches included linear spectral method, empirical transfer function,

local approximation methods, and local polynomial approximations had been examined numerically with the use of waves produced from Fourier method. He claimed that global approaches are less accurate compared to local approaches.

Floating structures e.g. semi-submersible were found contributed significantly to the oil and gas industry. Hassan et al. [19] established the results of their research conducted on forces and motions of both free floating and moored semi-submersible by using numerical computation method. Heidari et al. [20] compared the dynamic behavior of a moored semi-submersible between both type of waves under the effect of transverse phase lag and angle of incidence. They found that short-crested wave fields generate higher value in specific frequency and directions under the influence of different wave incidence angle.

Apart from that, Kurian et al. [21] had conducted similar experiment to investigate the motion responses of semi-submersible due to the effect of short-crested bi-directional waves crossing angle. In their study, they used multi-element wave generation system of the wave maker together with semi-submersible model to simulate multidirectional wave condition in the real ocean. They concluded that the magnitude and trend of dynamic responses can be influenced significantly by wave crossing angle.

Besides, Kurian et al. [22, 23, 24] had carried out a lot of researches regarding motion responses of floating offshore structures numerically and experimentally subjected to waves. They applied the Newmark Beta Method in time domain analysis to solve the equation of motions for the structure dynamic equilibrium and linear airy wave principle in numerical calculation to attain the wave properties data. They proved that short-crested waves yield smaller dynamic motion than long-crested waves in surge, heave, and pitch through both experiment and numerical study on truss spar. This finding can contribute to a more cost-effective and optimum design of deep water offshore platforms. In addition, they agreed that numerical simulation is applicable to offer similar results with experimental values. From the analysis of their results gained, it is found that the structures perform similarly, where the higher the frequency, the lower the dynamic responses obtained. Moreover, Montasir et al. [25] further studied and considered additional current force at two types of spar i.e. the classic and truss spar. Their results demonstrated that current can affect significantly to generate opposing results.

From the above reviews, most of the studies conducted by previous researcher on wave kinematics utilized Morison Equation to compute wave forces calculation on the flooded member of offshore structures, where it offers relatively more accurate outcomes. Apart from that, all of the analysis on the subject of short-crested waves yield back positive feedback that it helps to design for more economical offshore structures. The above mentioned literature reviews is able to provide good guidance and material on this research title.

Nevertheless, the dynamic responses of semi-submersible by comparing between short-crested and long-crested waves incorporated with current, have not been studied broadly whereby the studies reported mainly focused only on directional wave spectrum, wave kinematics, and vertical circular cylinder. Furthermore, studies had been conducted on spar instead of semi-submersible and without considering current environmental factor. Hence in this study, the effect of short-crested waves incorporated with current on the dynamic responses of semi-submersible is necessary to be quantified and qualified.

CHAPTER 3

METHODOLOGY / THEORY

As methodology for this study, response amplitude operator (RAO) was computed by using the results obtained from frequency domain method and wave energy spectrum. For more detailed, directional wave spectrum is the product of unidirectional wave spectrum and directional spreading function. Frequency domain refers to the mathematical calculations and computations with respect to frequency, instead of time. Thus, frequency domain analysis was executed by representing the density distribution of sea waves at the chosen deep-water region with an appropriate wave spectrum model. Then, RAO was simulated by using force components calculated. Lastly, the motion response spectrum was computed by using the wave spectrum and RAO for the responses in three degrees of freedom.

3.1 Structural Model and Coordinate System

All the locations in this project were specified based on the platform global axis system as shown in the figure below for the calculation of wave forces and moment.

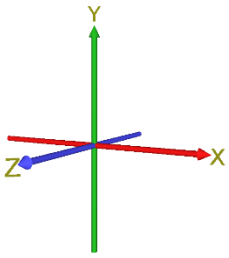

Figure 1: Coordinate System

An eight column semi-submersible model was used in this project calculation with scale factor of 1:100 and also Froude Scaling Law. The principle dimensions and details of the model were given as table below.

Table 1: Dimensions of Model

Variable	**Dimension**
Centre of gravity	(0,0)
Diameter of column 1, 4, 5, 8	0.10 m
Diameter of column 2, 3, 6, 7	0.06 m
Height of pontoon	0.10 m
Height of column	0.26 m
Distance of column 1&5 from (0,0)	-0.45 m
Distance of column 2&6 from (0,0)	-0.15 m
Distance of column 3&7 from (0,0)	0.15 m
Distance of column 4&8 from (0,0)	0.45 m
Total mass	42.83 kg
Significant Wave Height	1.40 m
Water depth	1200.00 m
Current	1.00 m/s
Natural Period for F_x	100.00 s
Natural Period for M_y	60.00 s
Natural Period for F_y	50.00 s

The model layout for this study was an eight-column semi-submersible is shown as follow:

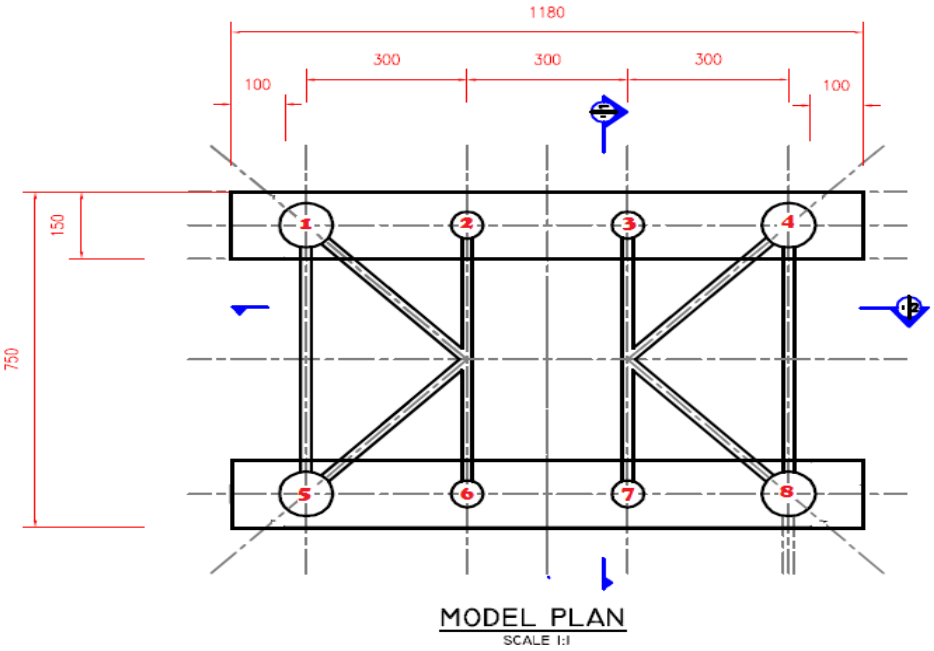

Figure 2: Eight-Column Semi-Submersible Model Plan 1

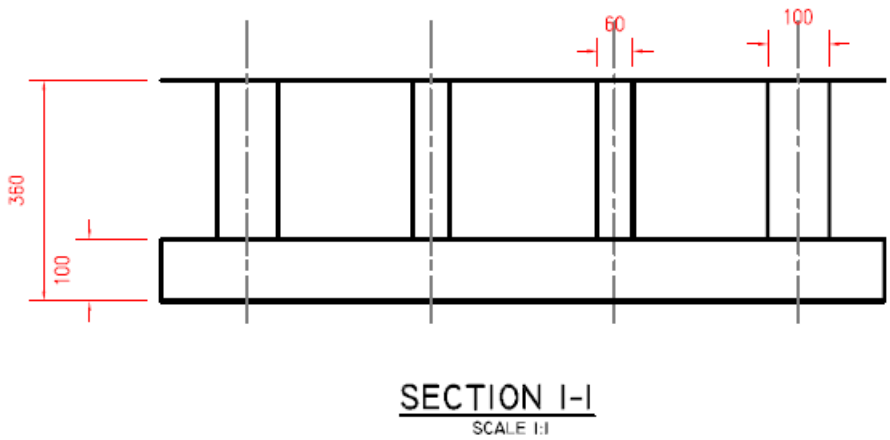

Figure 3: Eight-Column Semi-Submersible Model Plan 2

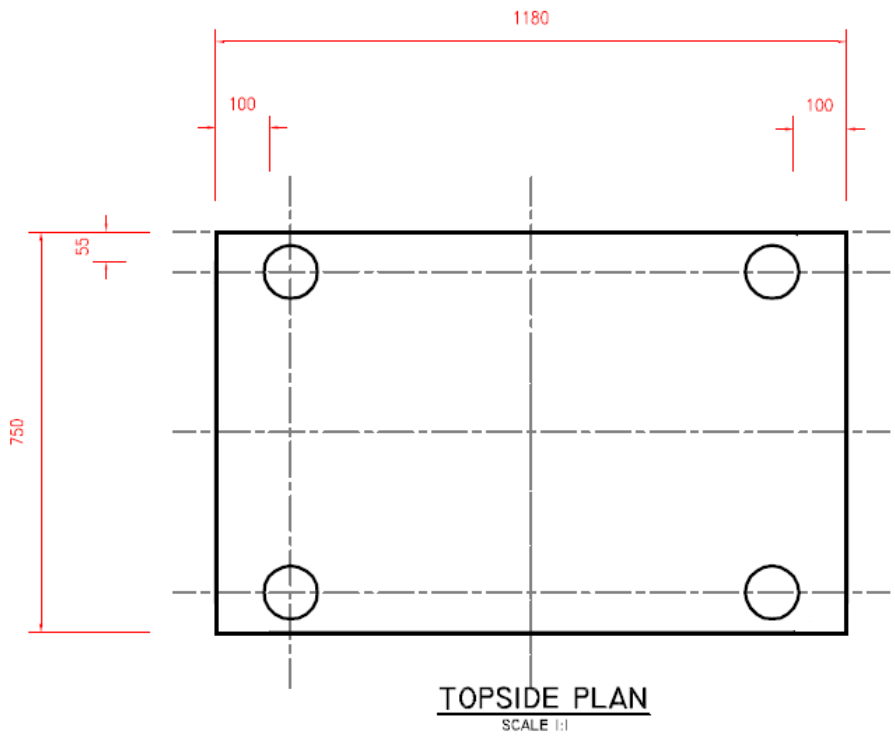

Figure 4: Eight-Column Semi-Submersible Topside Plan

3.2 Force Components

3.2.1 Morison Equation

Morison Equation was used for calculating the resultant horizontal wave force (F_T) acting on a vertical circular cylinder through the summation of drag force (F_D) and inertia force (F_I), which usually involved water particles velocity, acceleration, and displacement. The reason of considering F_I was due to the concept of water particle moves in a wave carried a momentum with it. On the other hand, F_D was needed to be considered due to the presence of pressure differential at the fore and aft of the vertical cylinder at a given time. The pressure differential caused a force to be exerted in the same direction of the instantaneous water particle velocity.

F_T obtained from Morison Equation represented the surge motion (F_x) ranged from wave period 0 second to 100 second and frequency 0 Hz to 0.5 Hz. Environmental criteria at

the region around Gumusut-Kakap field (water depth 1200m) had been proposed in the calculation of this project such as H_s in operating criteria.

Determination of horizontal wave forces as divided into four sections, column 1 and 5, column 2 and 6, column 3 and 7, column 4 and 8 because they encountered similar amount of forces. Horizontal forces exerted on the pontoon was not included in the computation because its orientation contributed only insignificant wave forces.

At each frequency, the forces obtained for every elevation were then summed up for 0 second to 100 second. Next, the maximum force was determined for every frequency and added up for total four sections to compute RAO.

The equation of Morison Equation was demonstrated as below:

$$F_D = \frac{1}{2} C_D D \rho u \, |u| \partial s \tag{1}$$

$$F_I = C_m \frac{\pi}{4} \rho D^2 \frac{\partial u}{\partial t} \partial s \tag{2}$$

$$F_T = \frac{1}{2} C_D D \rho u \, |u| + C_m \frac{\pi}{4} \rho D^2 \frac{\partial u}{\partial t} \tag{3}$$

$$u = \frac{\pi H_s}{T} \frac{\cosh ks}{\sinh kd} \cos \theta \tag{4}$$

$$\frac{\partial u}{\partial t} = \frac{2\pi^2 H_s}{T} \frac{\cosh ks}{\sinh kd} \sin \theta \tag{5}$$

Where F_T was wave force on a circular cylinder (N); C_D was dimensionless drag coefficient; C_M was dimensionless inertia coefficient; D was diameter of semi-submersible member (m); ρ was density of seawater (taken as 1040 kg/m^3); u was instantaneous horizontal water particle velocity (m/s); ∂u/∂t was horizontal local water particle acceleration at the centerline of the cylinder (m/s^2); H_s was significant wave height (m); T was wave period (s); L was wave length (m); ω was wave frequency (s^{-1}); k was wave number (m^{-1}); d was water depth (m); g was gravitational acceleration (given as 9.806 m/s^2); x was horizontal distance from center of gravity (m); t was time distant at which water particle kinematics was evaluated (s).

3.2.2 Vertical Force

The Pressure Area Theory was used to obtain heave force (F_z) exerted on pontoon of semi-submersible. It utilized multiplication of pressure and area where the pressure formula was shown as below:

$$p = \rho g \frac{H_S}{2} \frac{\cosh ks}{\cosh kd} \cos\theta \quad (6)$$

3.2.3 Moment Force

Pitch motion (M_y) was calculated by multiplying resultant force from Morison Equation (F_x) with level arm. Level arm was the vertical distance measured between the center of gravity and the resultant force from horizontal direction. For the model used in this project, its center of gravity was approximately 0.16m below topside.

3.2.4 The Total Force

Next, the F_x and M_y was calculated by adding in current induced using the formula:

$$F = \frac{1}{2} C_D D \rho (u + U) |u + U| + C_m \frac{\pi}{4} \rho D^2 \frac{\partial u}{\partial t} \quad (7)$$

Where U was current at surface (m/s).

3.3 Wave Spectrum and Directional Wave Spectrum

3.3.1 Wave Spectrum

Pierson-Moskowitz Spectrum, which was also identified as P-M Model, was proposed to be adopted for this study. This spectrum had been extensively investigated and applied by ocean engineers and offshore structures design applications as one of the most representative for water characteristics. This spectrum was used to simulate severe storm wave encountered by engineering structures in offshore. The P-M Spectrum, S(f) was expressed in terms of frequency (ranged from 0 Hz to 0.5 Hz) as below:

$$S(f) = \frac{ag^2}{(2\pi)^4} f^{-5} \exp\left[-1.25\left(\frac{f}{f_0}\right)^{-4}\right] \quad (8)$$

Where f_0 was peak frequency (s^{-1}).

3.3.2 Directional Wave Spectrum

For short-crested waves, its directional distribution was demonstrated by a cosine power law. The common form of short-crested waves was a cosine-squared distribution of the directional long-crested wave energy density distribution in the range of ±90° from the average wave direction. Therefore, the energy density was in a function of the frequency and direction as shown below, about a mean heading angle of waves.

$$S(f,\theta) = \frac{2}{\pi} S(f) cos^2\theta, \qquad -\frac{\pi}{2} \leq \theta \leq \frac{\pi}{2} \quad (9)$$

3.4 Motion Response Spectrum and RAO

The dynamic responses of semi-submersible under the effect of F_x, F_z, and M_y wave and current loadings were computed by using the formula below. RAO was computed after obtaining the force components and its method of calculation was similar for both long-crested and short-crested waves. To obtain the motion response spectrum, for long-crested waves, S(f) was represented by the wave spectrum from P-M model whereas for short-crested waves, S(f) was represented by the directional wave spectrum covering the range of ±90o. Thus, the graph was plotted to compare between wave spectrum and directional wave spectrum.

$$S_x(f) = RAO^2 * S(f) \quad (10)$$

$$RAO = \frac{F/(\frac{H_S}{2})}{[(K-mw^2)^2+(Cw)^2]^{1/2}} \quad (11)$$

Where K was stiffness of structure; m was mass of the structure; C was structural damping ratio.

3.5 Wave Profile and Motion Response

3.5.1 Wave Profile

The wave profile for multidirectional waves was obtained by considering random number generated from Microsoft Excel as below.

$$H(f) = 2\sqrt{2 * S(f) * \Delta f} \quad (12)$$

$$n(x,t) = \sum_{n=1}^{N} \frac{H(f)}{2} \cos[k(n)x - 2\pi f(n)t + \varepsilon(n)] \quad (13)$$

Where H(f) was wave height; epsilon was random number generated from Microsoft Excel; x=0m.

3.5.2 Motion Response

To compute the motion response, the following equation was used where RAO for F_x, F_z, and M_y wave and current were taken into account. H(f) was obtained by using wave spectrum or directional wave spectrum depending on the type of waves.

$$n(x,t) = \sum_{n=1}^{N} \frac{RAO * H(f)}{2} \cos[k(n)x - 2\pi f(n)t + \varepsilon(n)] \quad (13)$$

Lastly, the maximum amplitude from motion response was determined for comparison of dynamic responses among long-crested and short-crested waves, with and without current effect.

3.6 Key Milestone

The table below shows the key milestone for this entire project.

Table 2: Key Milestone for Final Year Project I & II

Week	Final Year Project I Milestone
1	Able to select and confirm project title
9	Able to complete all the calculations for wave spectrum (P-M Spectrum and Jonswap Spectrum)
11	Able to complete all the calculations for long-crested waves (F_x, F_z, and M_y)
13	Able to complete all the calculations incorporated both long-crested waves and current (F_x and M_y)
Week	**Final Year Project II Milestone**
1	Able to start up with directional wave spectrum by using MATLAB code
6	Able to complete all the calculations for short-crested waves (F_x, F_z, and M_y)
8	Able to complete all the calculations incorporated both short-crested waves and current (F_x and M_y)
10	Able to compute and complete all numerical comparative study between long-crested and short-crested waves for entire project

3.7 Gantt Chart

The table below shows the Gantt-Chart for this entire project.

Table 3: Gantt-Chart for Final Year Project I & II

Activities	Final Year Project I (Week No.)													
	1	2	3	4	5	6	7	8	9	10	11	12	13	14
Selection and Confirmation of Project Title														
Understanding & Computation of Wave Spectrum														
Understanding & Computation of Morison Equation for F_x														
Preparation & Submission of Extended Proposal														
Understanding & Computation of Pressure Area Theory for F_z														
Understanding & Computation of Theory for M_y														
Understanding & Computation of Long-Crested Wave and Current														
Proposal Defense & Progress Evaluation														
Preparation & Submission of Draft Interim Report														
Preparation & Submission of Final Interim Report														
Activities	**Final Year Project II (Week No.)**													
	1	**2**	**3**	**4**	**5**	**6**	**7**	**8**	**9**	**10**	**11**	**12**	**13**	**14**
Calculation of Short-Crested Wave using MATLAB Code														
Calculation of RAO and Numerical Comparative Study														
Preparation & Submission of Progress Report														
Final Computation and Checking on Calculations and Results														
Poster Design & Pre-SEDEX														
Preparation & Submission of Draft Project Dissertation														
Preparation & Submission of Technical Paper & Final Project Dissertation (Soft Bound)														
Viva & Submission of Final Project Dissertation (Hard Bound)														

CHAPTER 4

RESULTS AND DISCUSSION

4.1 Force Components

By using the methodology mentioned in previous section, results had been obtained and presented in term of graphs for better illustration purposes. The dynamic responses for all the three degrees of freedom, i.e F_x, F_z, and M_y due to long-crested and short-crested waves together with current were obtained. The total forces and moment obtained due to long-crested waves were illustrated in Figure 5 to Figure 7, where the graphs demonstrated that same wave height and wave period were repeated with respect to time.

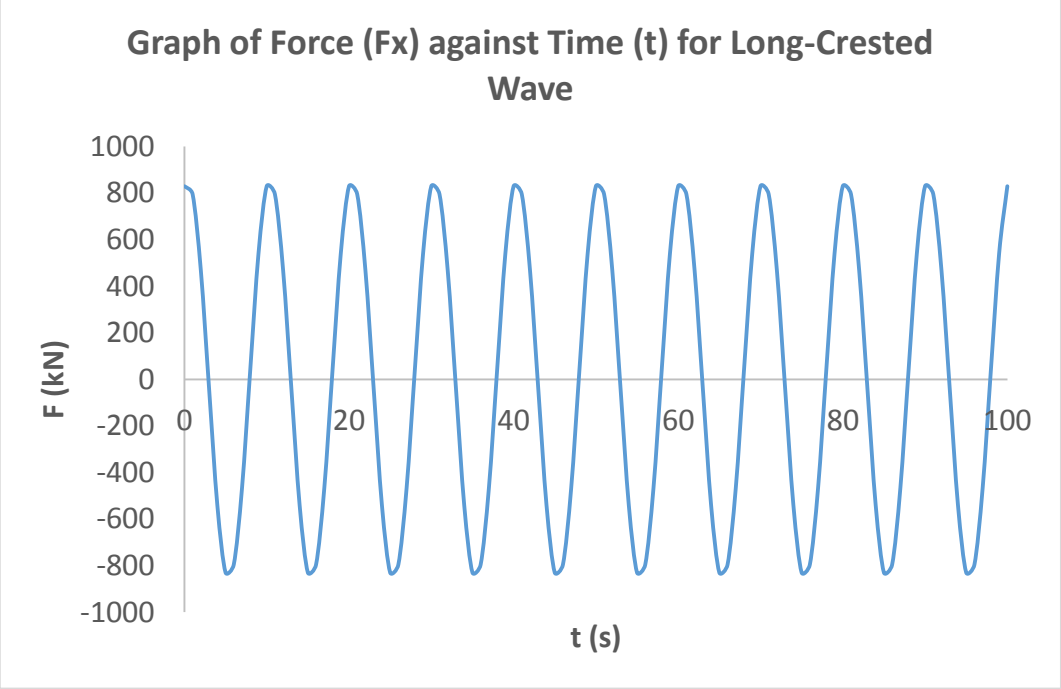

Figure 5: Graph of Force (F_x) against Time for Long-Crested Wave

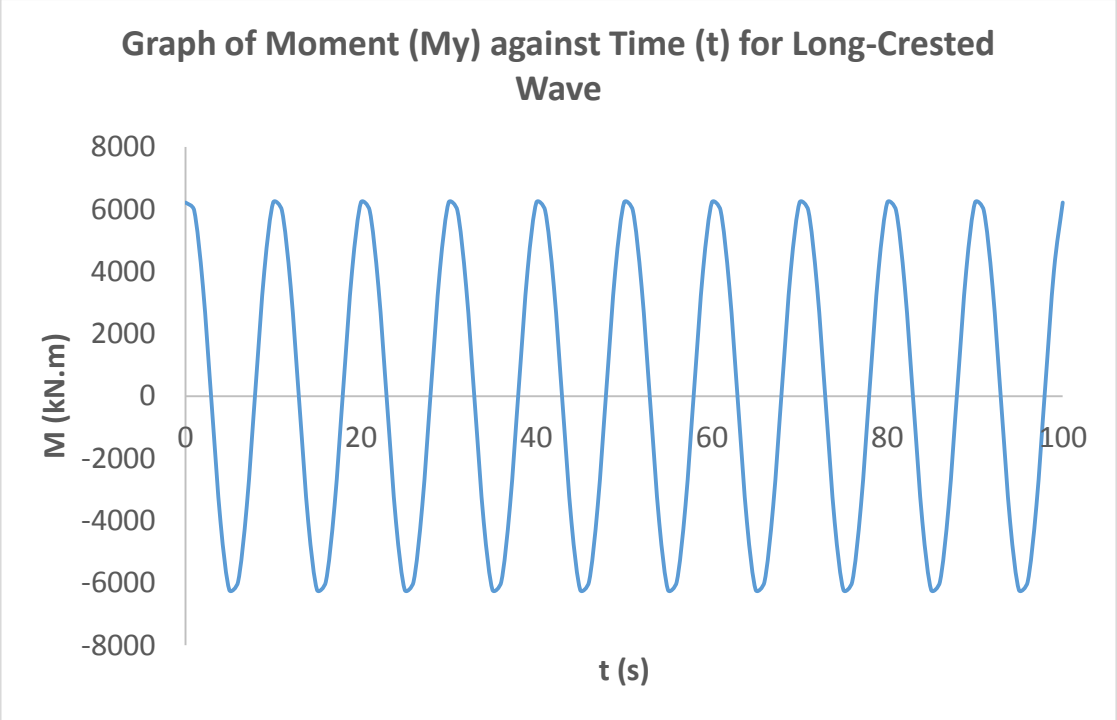

Figure 6: Graph of Moment (M_y) against Time for Long-Crested Wave

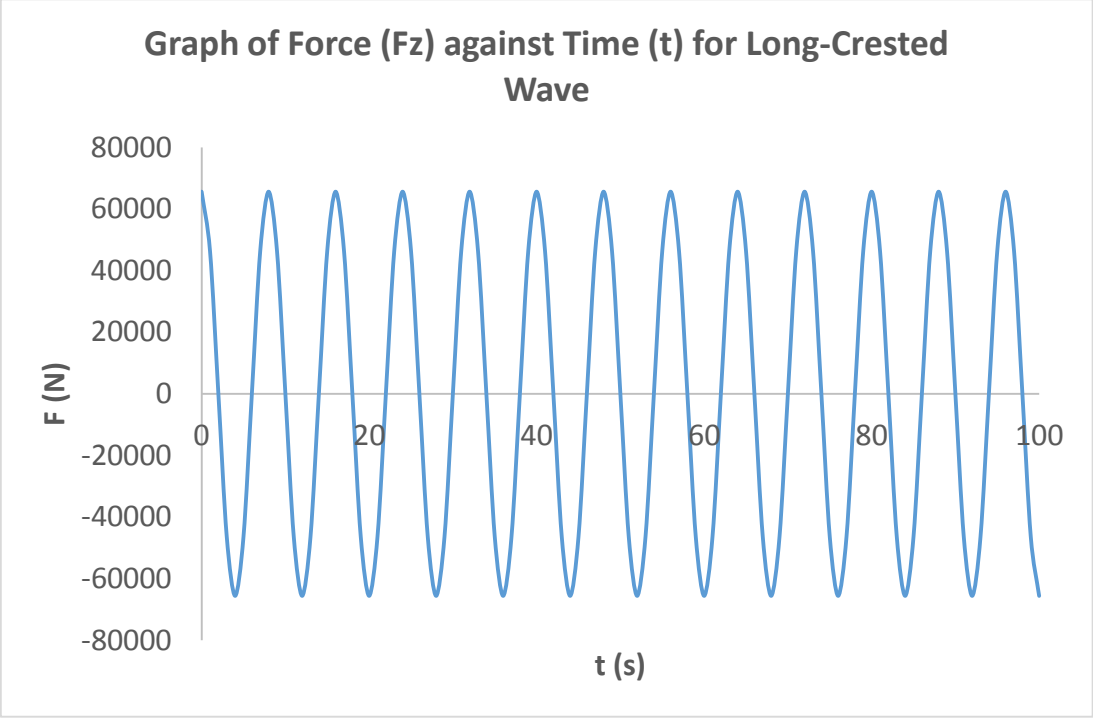

Figure 7: Graph of Force (F_z) against Time for Long-Crested Wave

According to the results obtained, it was noticeable that greater value of outcome was obtained from column 1, 4, 5, and 8 for each degree of freedom in accordance to the arrangement in model layout (Figure 2 to Figure 4). The four columns withstood almost similar values of F_x and M_y forces, but it was relatively larger compared to the rest of the columns. In another words, most of the wave forces were taken by column 1, 4, 5, and 8 as they were located at the outer corner of semi-submersible model which experiencing most of the waves trigger. Thus, those columns were designed to possess bigger diameter as the main support of the model.

Comparing F_x and F_z results, the pontoon of the semi-submersible model encountered insignificant wave force as F_z was the smaller wave force acting vertically from the bottom of model while F_x was the horizontal force acted on the eight columns of model. On the other hand, this was interpreted that F_z motion was rather insignificant as compared to F_x and M_y motion. Due to large magnitude of wave and current loadings exerted on the columns, large moment was induced resulting bigger value of M_y and this brought along higher risk and trigger. In the meanwhile, the direction of moment was determined by the direction of horizontal wave forces acting on the columns.

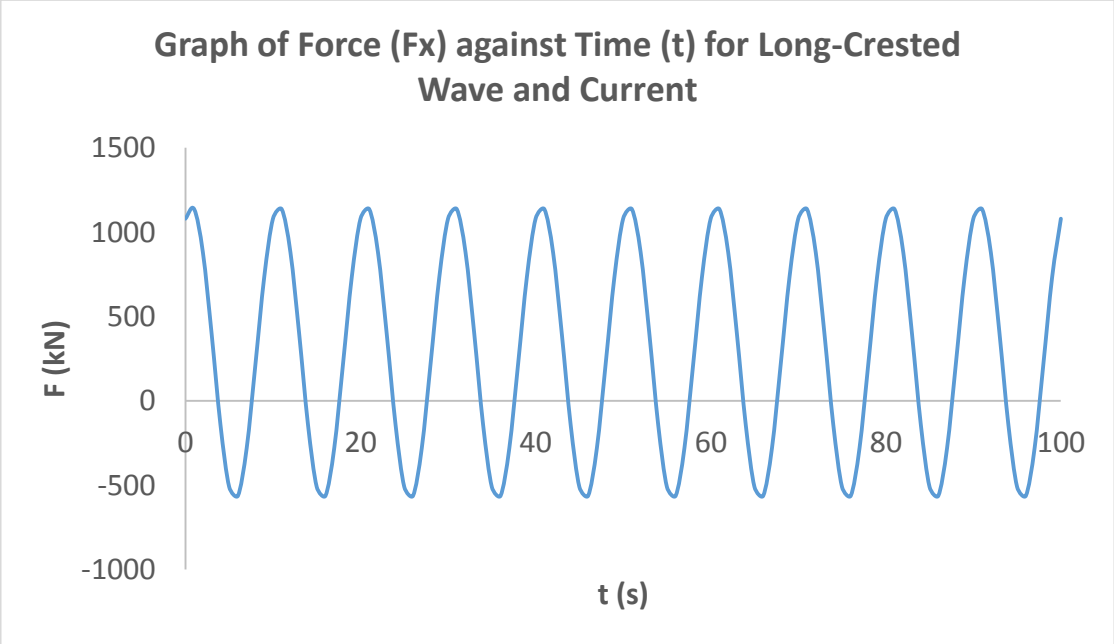

Figure 8: Graph of Force (F_x) against Time for Long-Crested Wave and Current

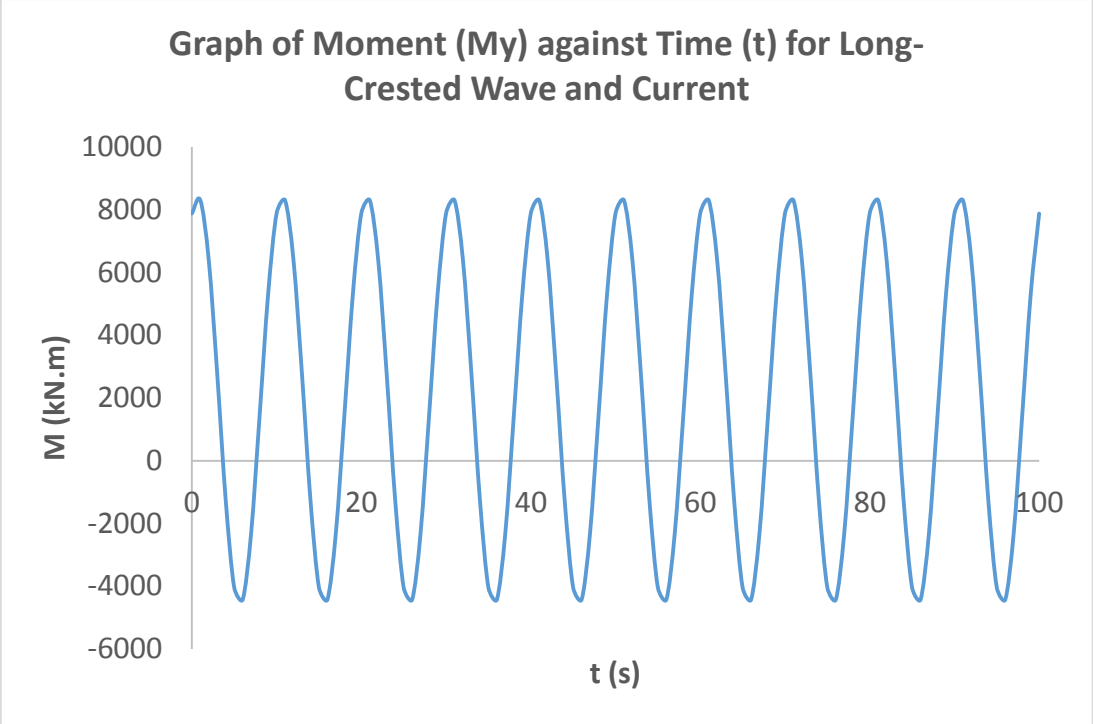

Figure 9: Graph of Moment (M_y) against Time for Long-Crested Wave and Current

F_x and M_y motion subjected to long-crested waves with current were illustrated in Figure 8 and Figure 9. The magnitude as well the trend of graphs for considering both long-crested wave and current induced were similar to the one considering the long-crested wave only. A difference of only 20% and 27% were observed in the comparison for M_y and F_x respectively. This was mainly due to the insignificant effect of current induced to the dynamic responses of semi-submersible as compared to wave forces. This was also supported by the statistics established that waves constituted 70% of major offshore environmental forces.

4.2 Wave Spectrum and Directional Wave Spectrum

4.2.1 Wave Spectrum

The graph of wave energy density spectrum, S(f) had been plotted based on P-M and Jonswap Spectrum as shown below Figure 10. From the graph, it was found that the peak frequency (maximum peak value) for Jonswap Spectrum was 2 times higher than P-M Spectrum, 24.4 m^2s and 11.8 m^2s respectively at the same frequency, 0.1 Hz. This was due to Jonswap Spectrum considered more parameters such as shape parameter and peakedness parameter, compared to P-M Spectrum. Therefore, Jonswap Spectrum was selected commonly for more conservative design, which could bring lower risk. Theoretically, the total energy of wave was represented by the area covered under the energy density curve in the graph.

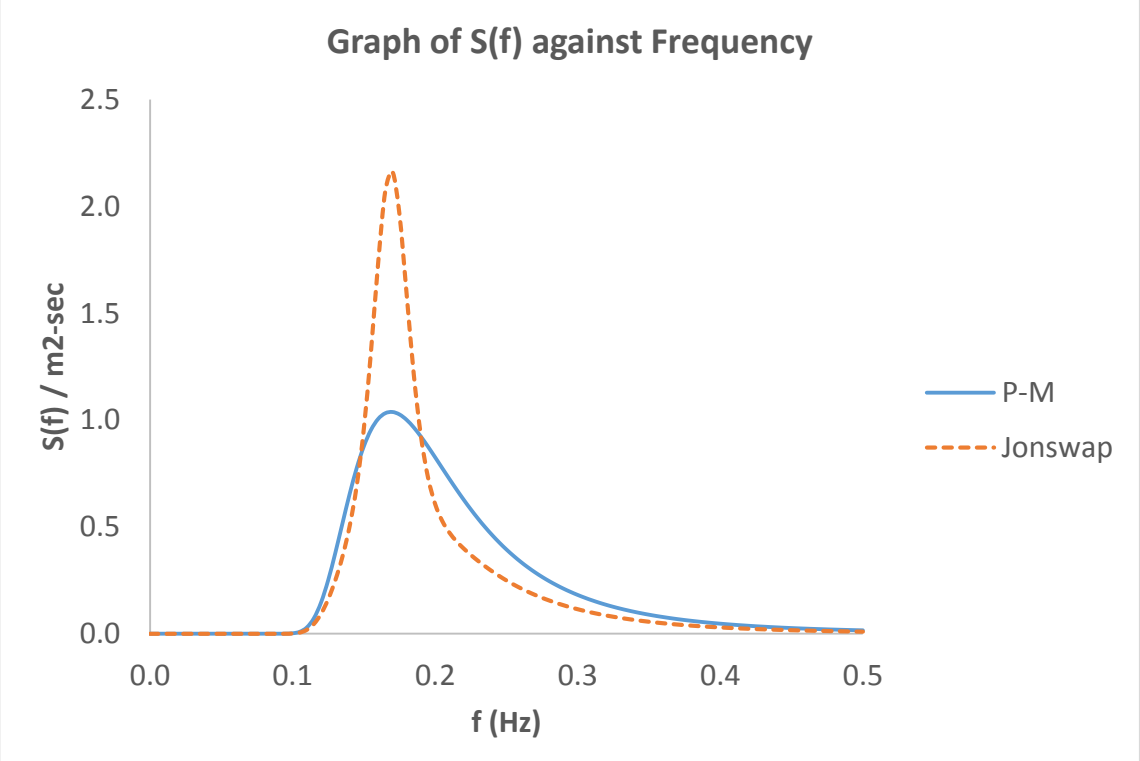

Figure 10: Comparison between P-M and Jonswap Spectrum

4.2.2 Directional Wave Spectrum

Figure 11 disclosed the comparison between wave spectrum and directional wave spectrum, where directional wave spectrum had taken the effect of direction of wave propagation into consideration. From the graph, it was observed that the wave spectrum from the P-M model was nearly one fourth of the peak value of directional wave spectrum. The values of these spectrums then affected considerably to the maximum amplitude of motion response when comparing between long-crested and short-crested waves.

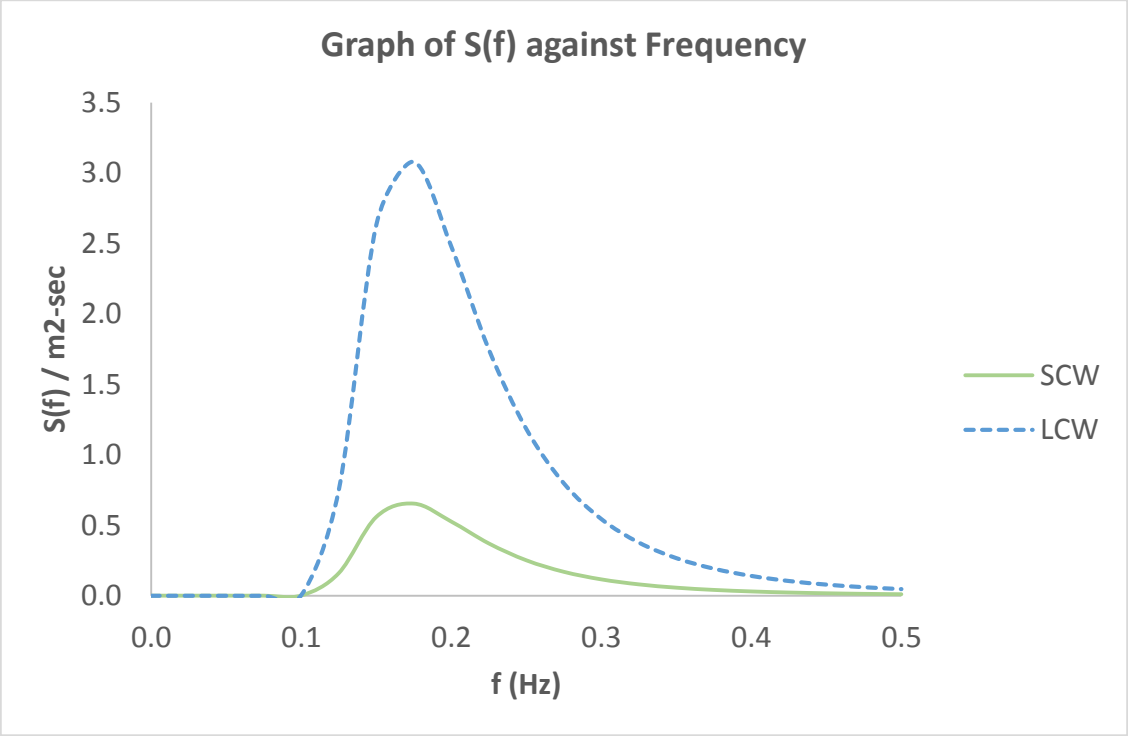

Figure 11: Comparison between Wave Spectrum and Directional Wave Spectrum

4.3 Motion Response Spectrum and RAO

The motion response spectrum and RAO had been computed, as shown in the following section for each degree of freedom analyzed. For the computation of RAO, the maximum wave forces and moment obtained from Morison Equation and other theories mentioned were inserted into the RAO formula. Next, square of RAO was then multiplied with P-M spectrum S(f) for each frequency between 0 Hz to 0.5 Hz to get motion response spectrum, $S_x(f)$ for each degree of freedom: F_x, M_y, and F_z.

4.3.1 RAO

RAO was used to determine the potential behavior of an offshore structure would possess when operating at sea. According to the RAO graph obtained (Figure 12 to Figure 16), it showed the trend, where the RAO decreased in corresponding to the increase of frequency. The magnitudes of RAO were found significantly varied at low frequency range, which caused by the non-linearity occur in the low frequency range. The RAO value for M_y subjected to waves and current was higher, which was 20 degree per meter. However, the RAO results of M_y motion with current exceeded the acceptable range in real case situation while the others were satisfactory for ordinary ocean circumstance, which were around 0.35m/m to 4deg/m. This was most probably due to the environmental loadings were taken from deep-water region, resulting in higher RAO values. From Figure 17 and Figure 18, it indicated that the effect of considering only wave loadings were approximately 20% of the RAO subjected to waves incorporated with current for both F_x and M_y.

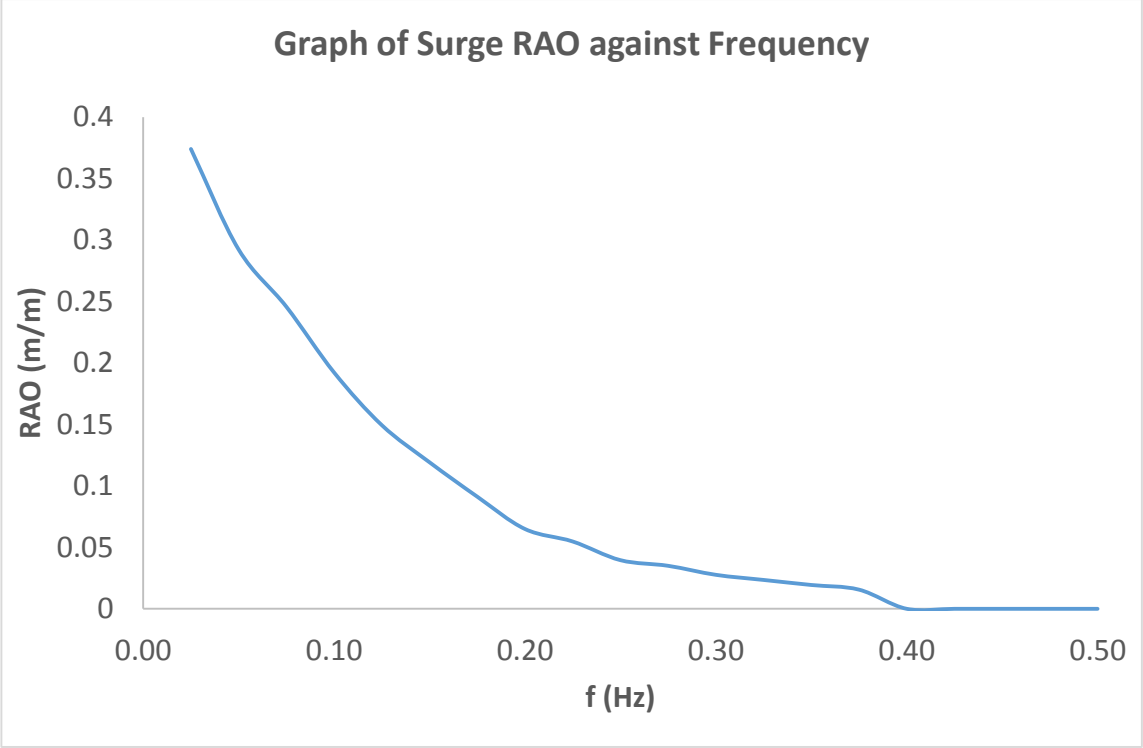

Figure 12: Graph of RAO (F_x) against Frequency

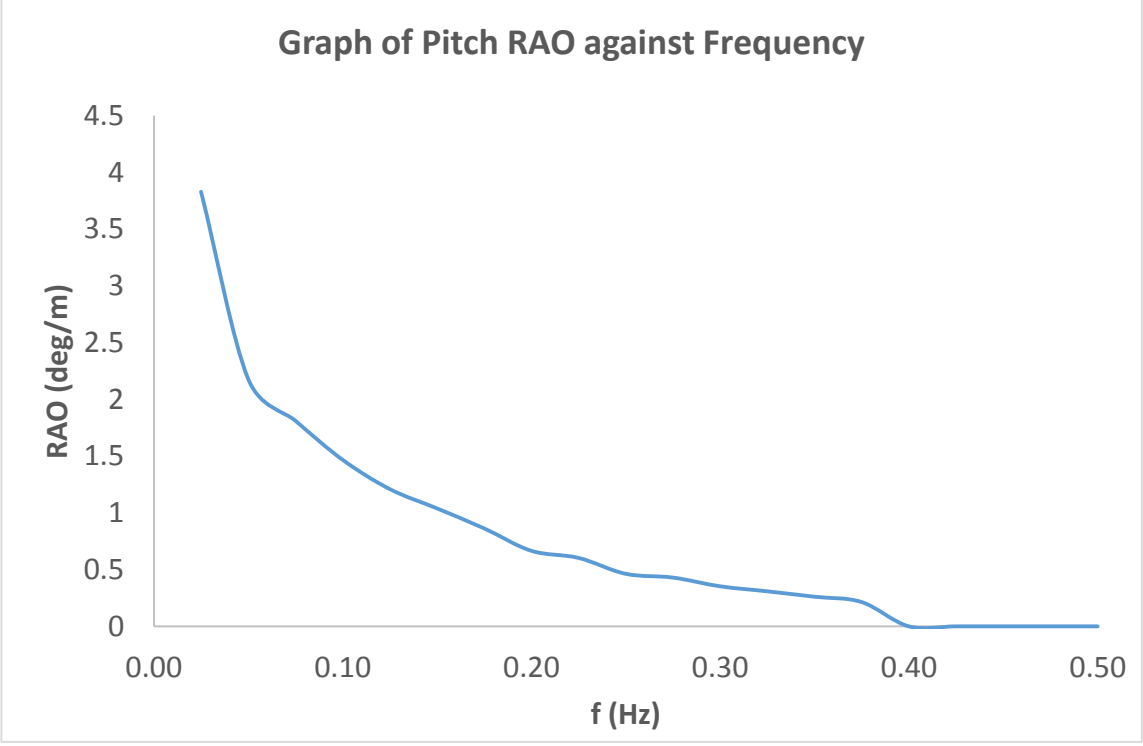

Figure 13: Graph of RAO (M_y) against Frequency

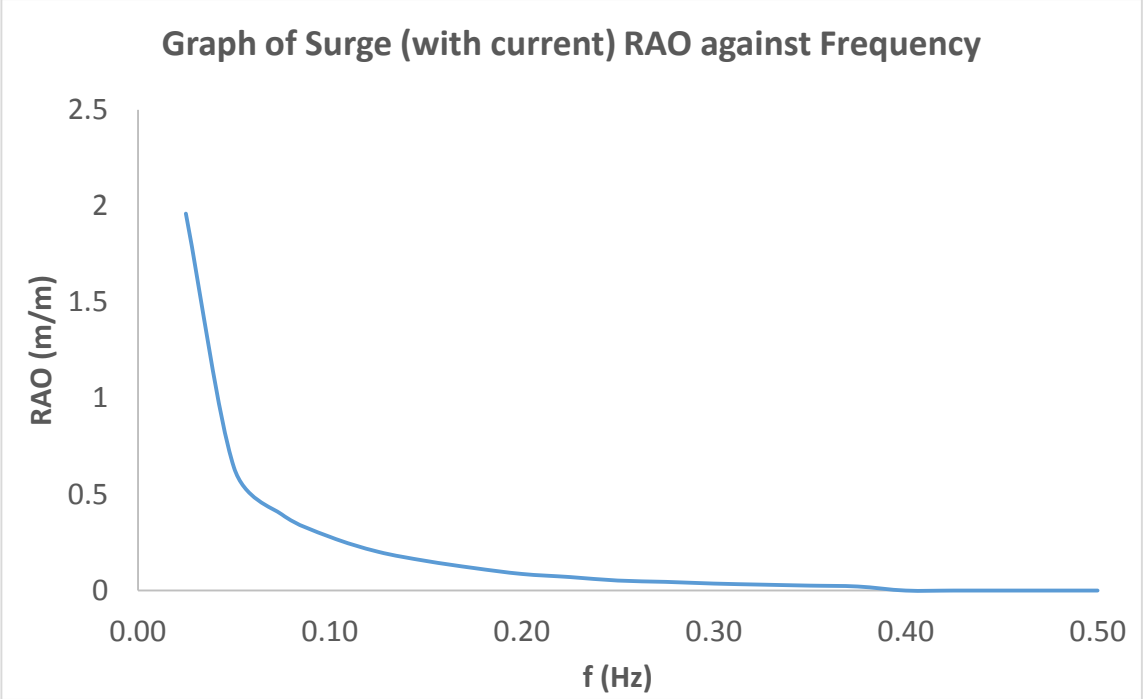

Figure 14: Graph of RAO (F_x with current) against Frequency

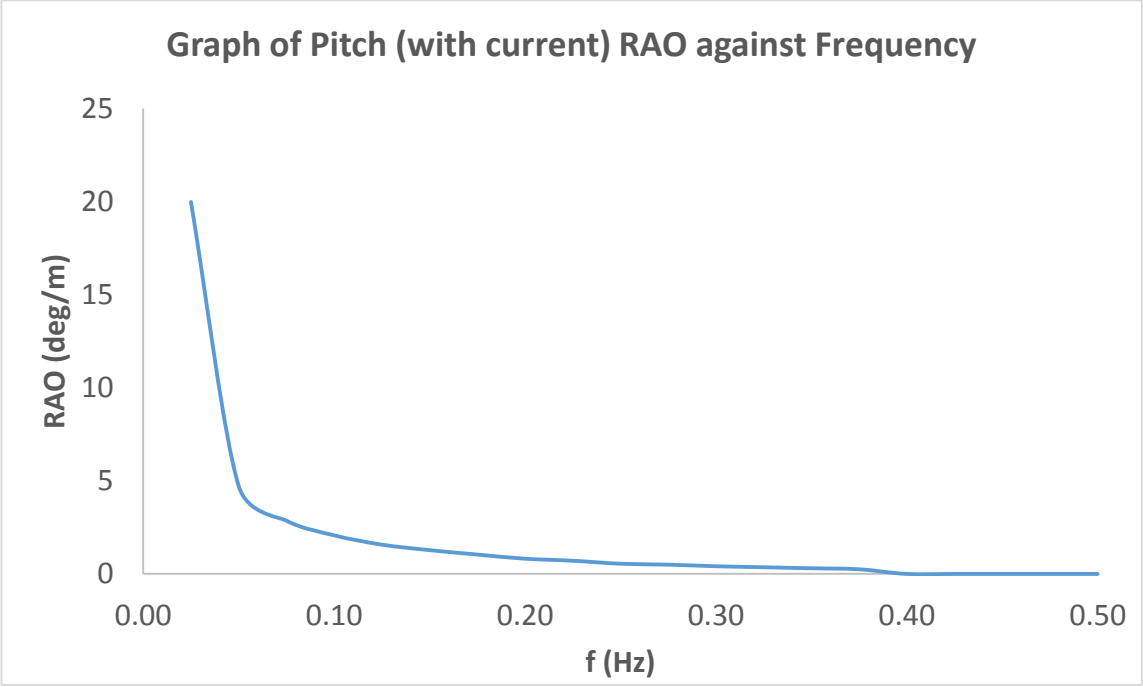

Figure 15: Graph of RAO (M_y with current) against Frequency

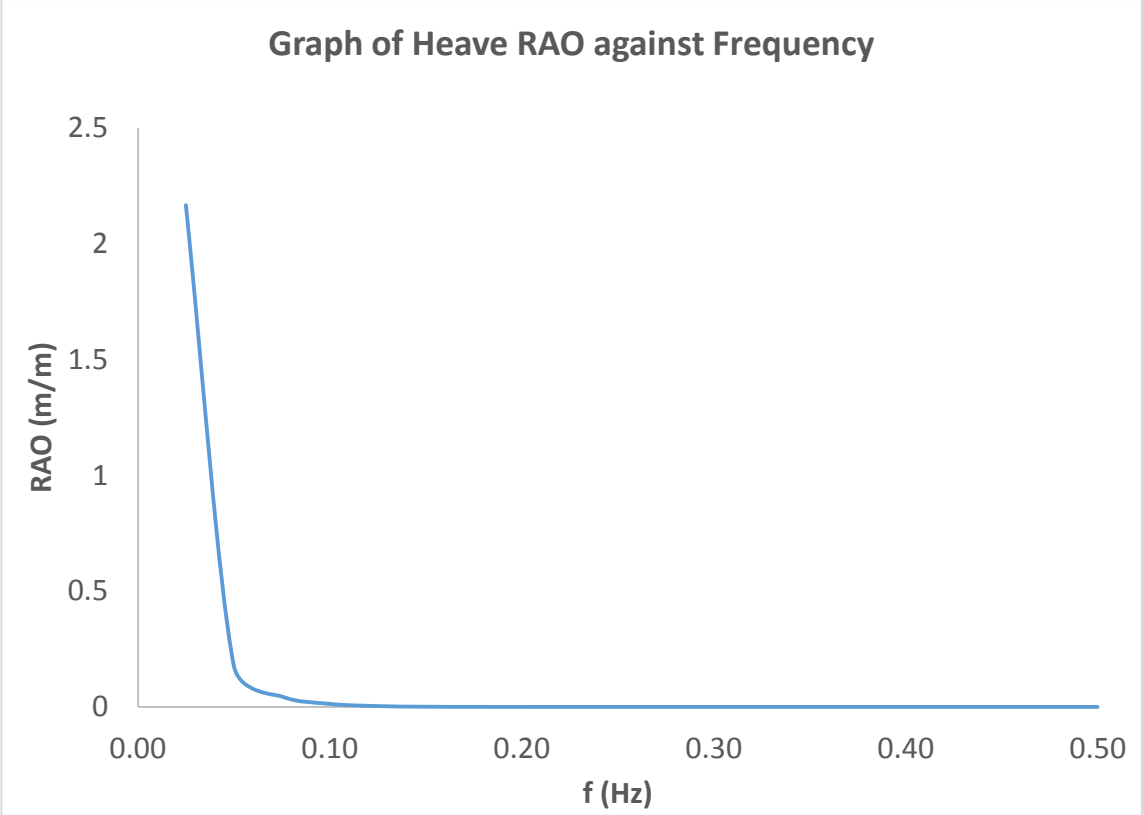

Figure 16: Graph of RAO (F_z) against Frequency

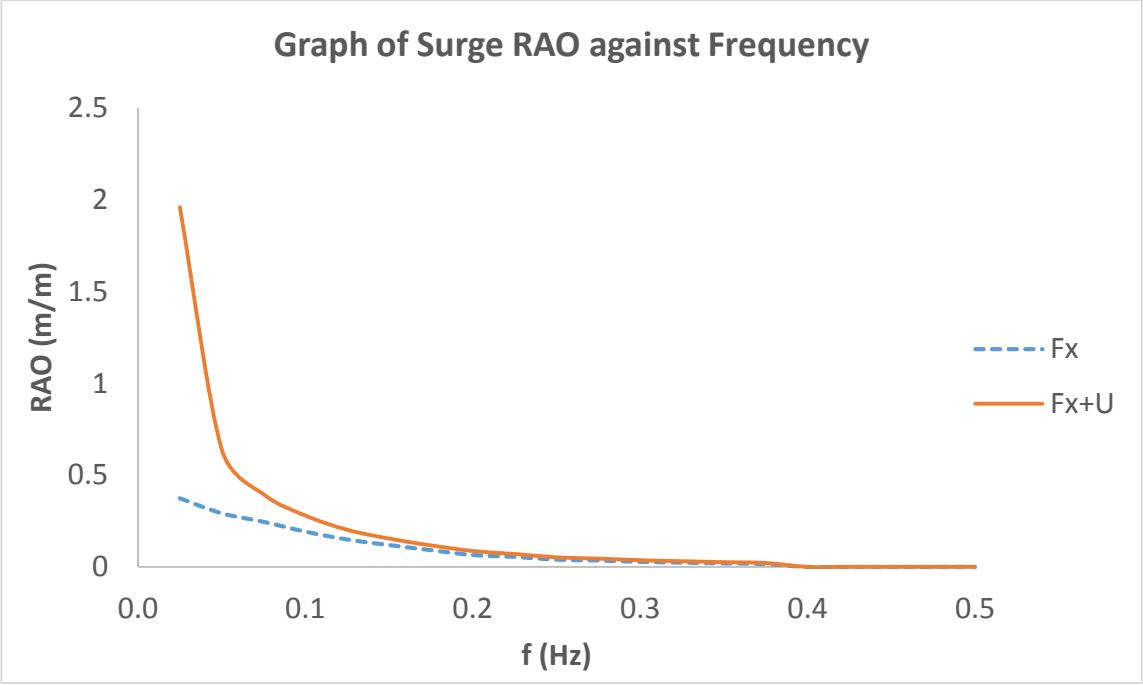

Figure 17: Comparison between F_x and F_x with Current

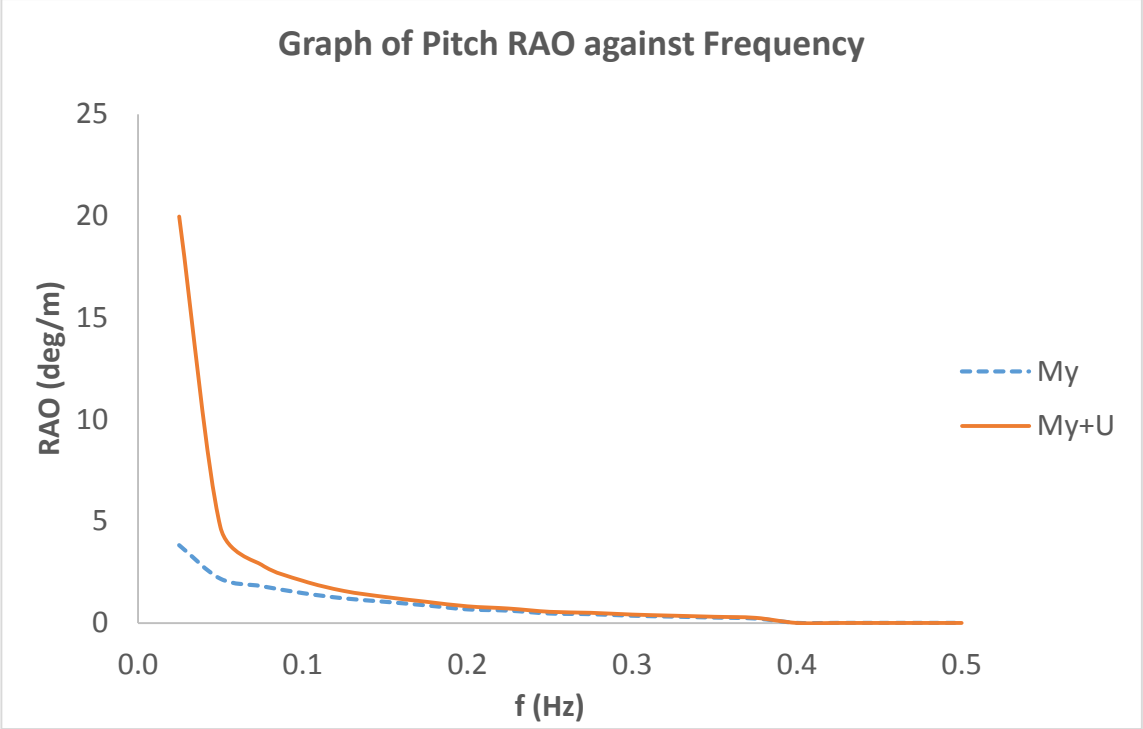

Figure 18: Comparison between M_y and M_y with Current

4.3.2 Motion Response Spectrum

As shown in the Figure 19 to Figure 23 were the comparison of $S_x(f)$ values between long-crested and short-crested waves. The peak energy for all degrees of freedom were observed at approximately 0.15 Hz frequency. However, significant variation was found in the magnitudes between the frequencies of 0.1 Hz and 0.3 Hz. In general, the peak values of short-crested waves were nearly four to six times lower than long-crested waves as it was mainly governed on the results of wave spectrum. RAO values were same for both types of waves causing no effect during comparison between long-crested and short-crested waves, but it influenced the results when comparing between degrees of freedom. Similar to force component graphs, $S_x(f)$ for M_y, which incorporated both wave and current effect, owned the highest peak value among the others due to the greatest value of force obtained. The area covered under the motion response spectrum curve for F_z was relatively smaller compared to the others as the total energy of waves exerted was smaller in that degree of freedom. In overall, F_z had the lower value, followed by F_x without current effect, F_x with current effect, M_y without current effect, and lastly was M_y with current effect.

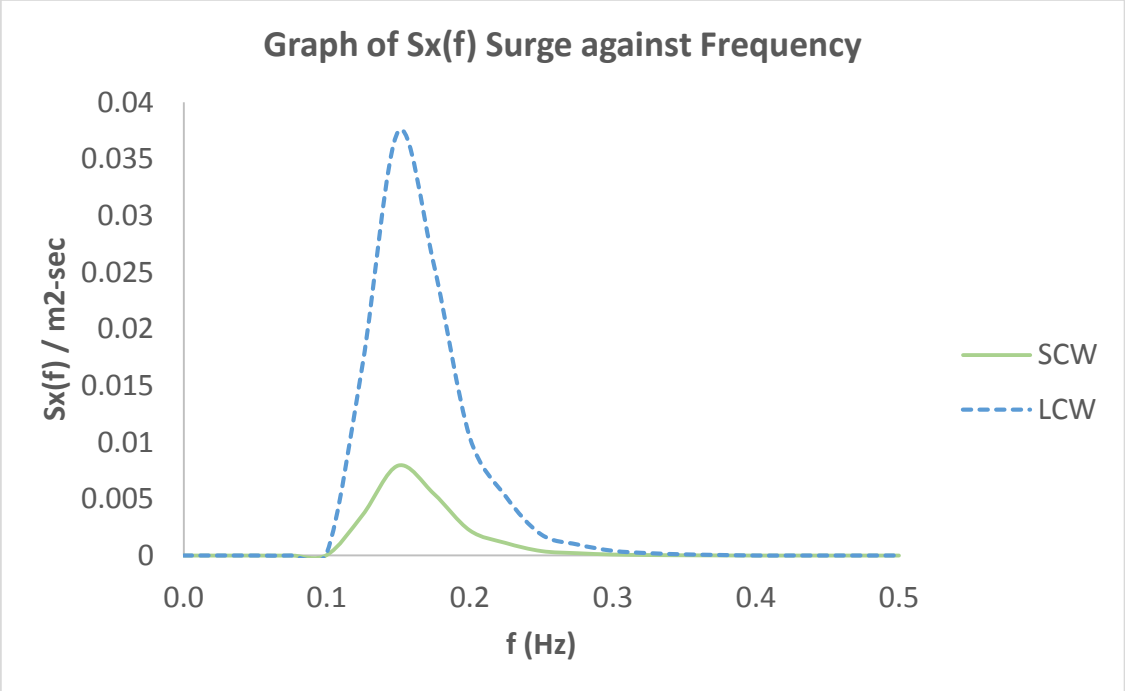

Figure 19: Graph of Motion Response Spectrum (F_x) against Frequency

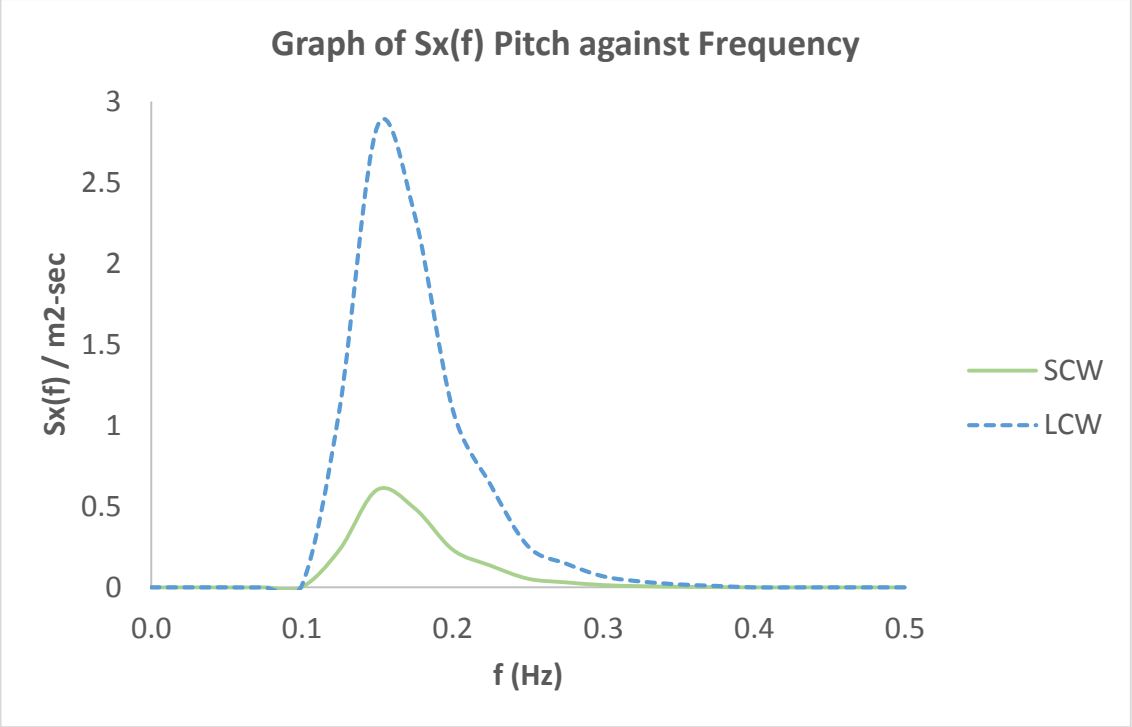

Figure 20: Graph of Motion Response Spectrum (M_y) against Frequency

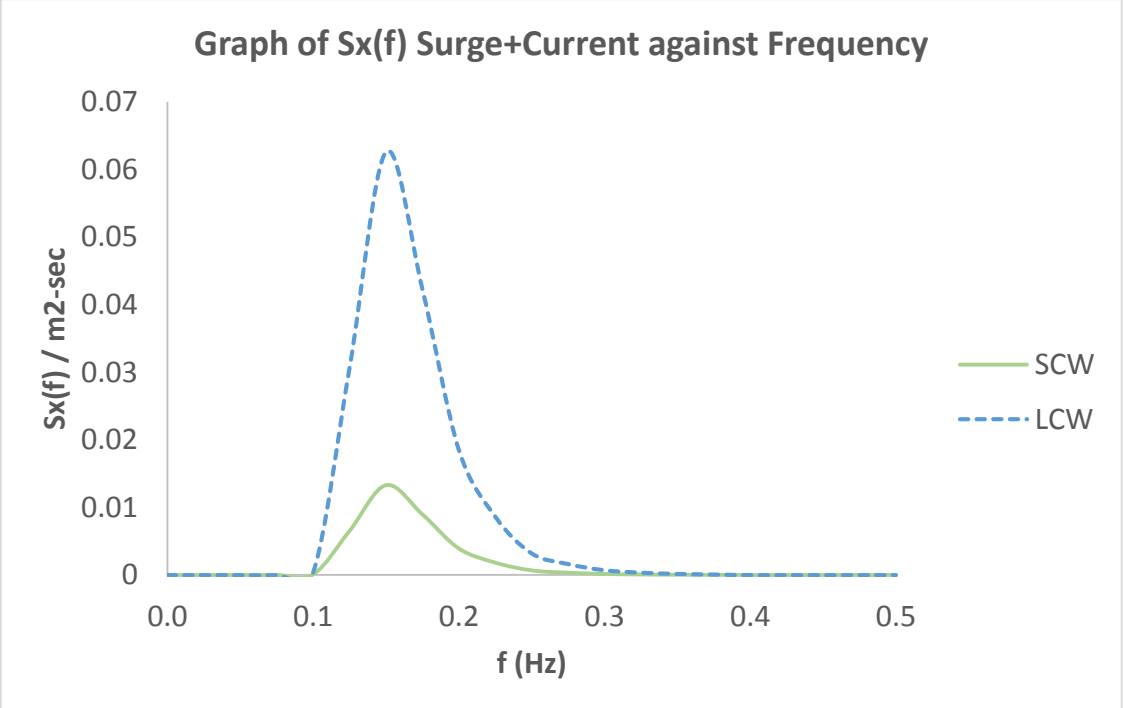

Figure 21: Graph of Motion Response Spectrum (F_x with current) against Frequency

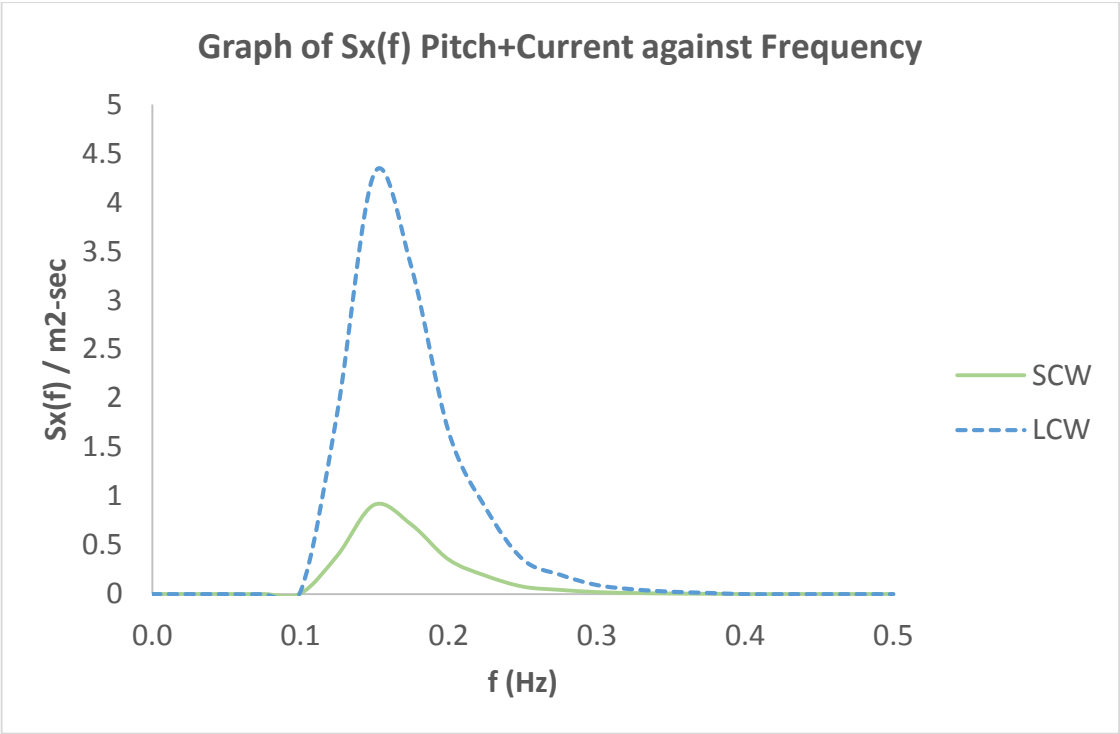

Figure 22: Graph of Motion Response Spectrum (M_y with current) against Frequency

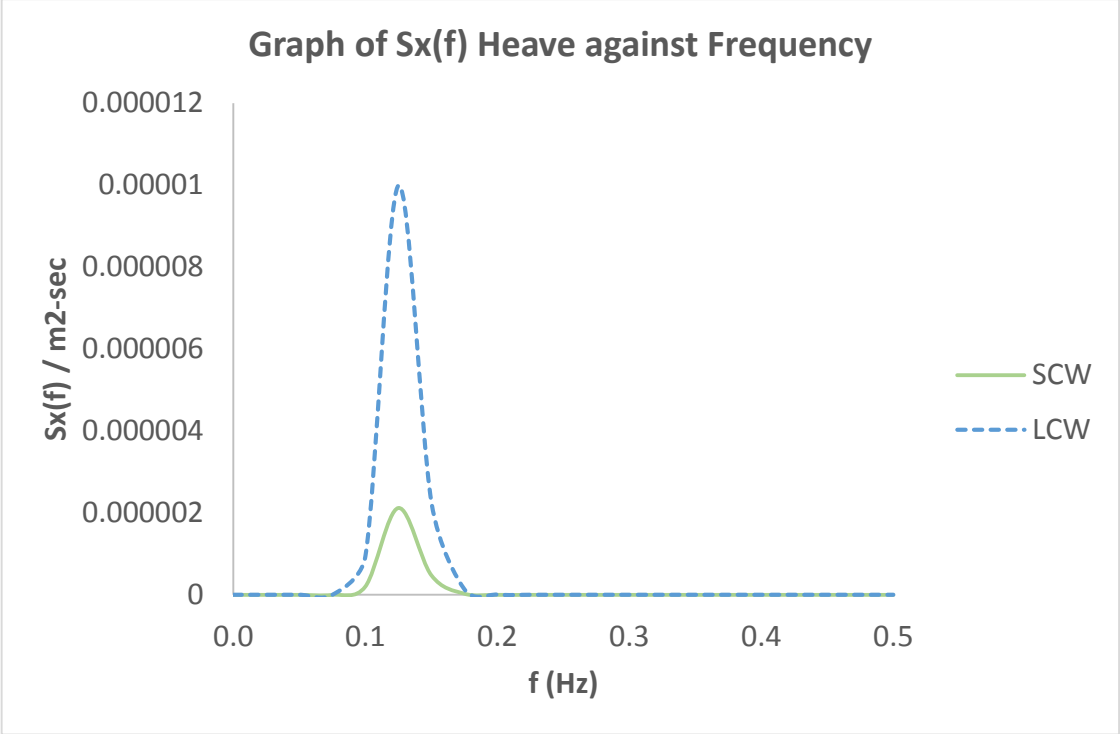

Figure 23: Graph of Motion Response Spectrum (F_z) against Frequency

4.4 Wave Profile and Motion Response

4.4.1 Wave Profile

The corresponding wave height from each frequency was then computed with reference to the above wave spectrum graph to generate the wave profile (t=0sec to t=100sec) at x=0m (initial position) to simulate the multidirectional wave at real sea condition (Figure 24). Random number generated from Excel formulation (between the ranges of 0 to 1) was utilized to retain the randomness of the time history in nature. Thus, the wave profile showed irregular and non-repeating pattern for every second. The highest wave height obtained from the stimulated wave profile was approximately 0.6 m.

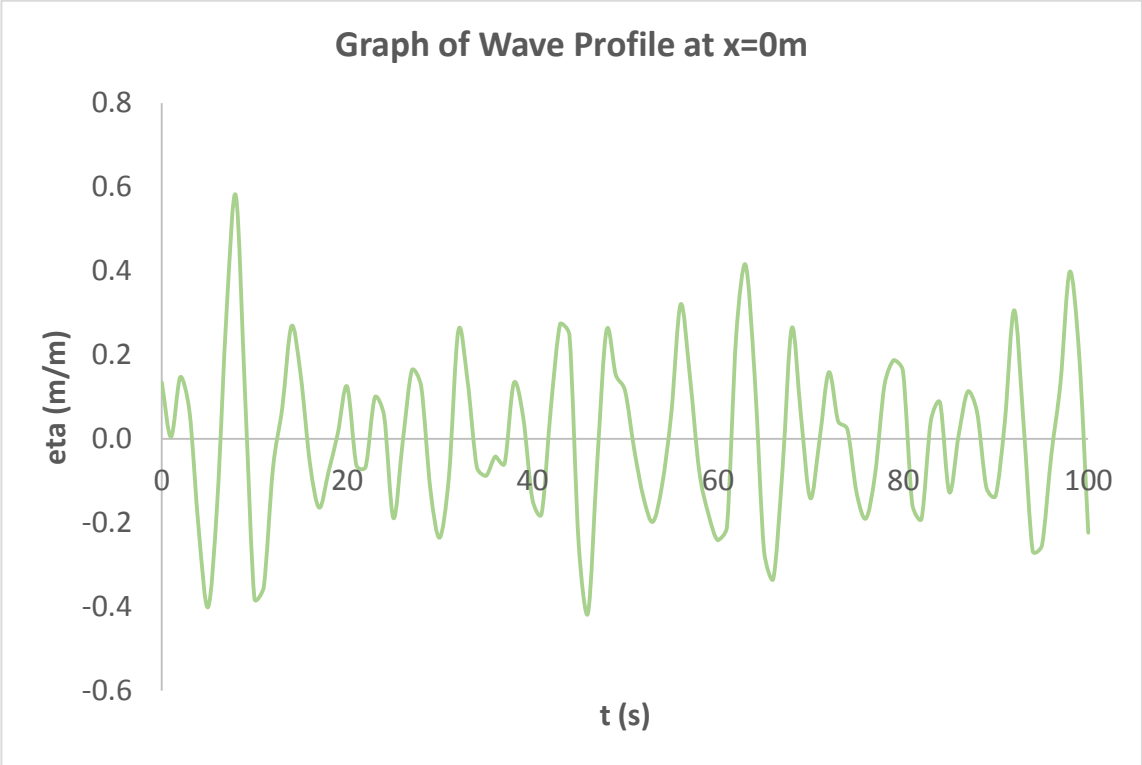

Figure 24: Graph of Wave Profile for Multidirectional Wave against Time at x=0m

4.4.2 Motion Response

Motion response had been computed for both long-crested and short-crested waves incorporated with current in three degrees of freedom. For illustration purpose, motion response graphs from long-crested and short-crested waves were presented below, where irregular waves were obtained. The difference between both types was mainly due to the influence of wave spectrum and directional wave spectrum.

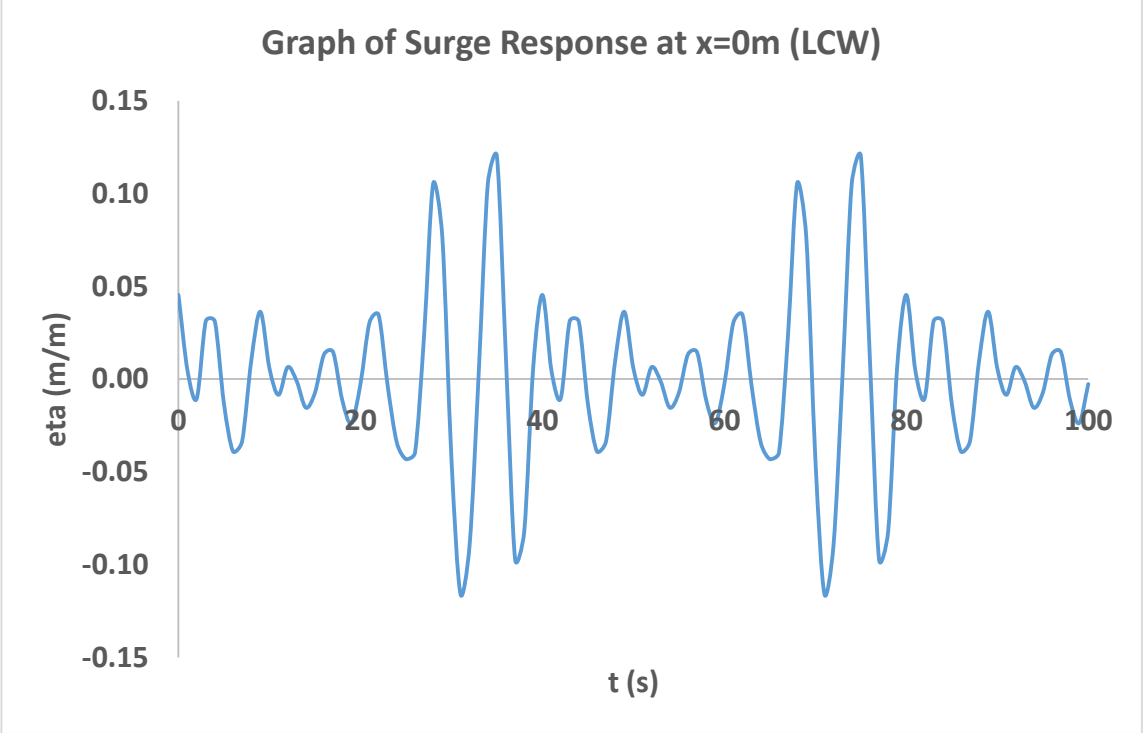

Figure 25: Response of F_x Motion for Long-Crested Waves

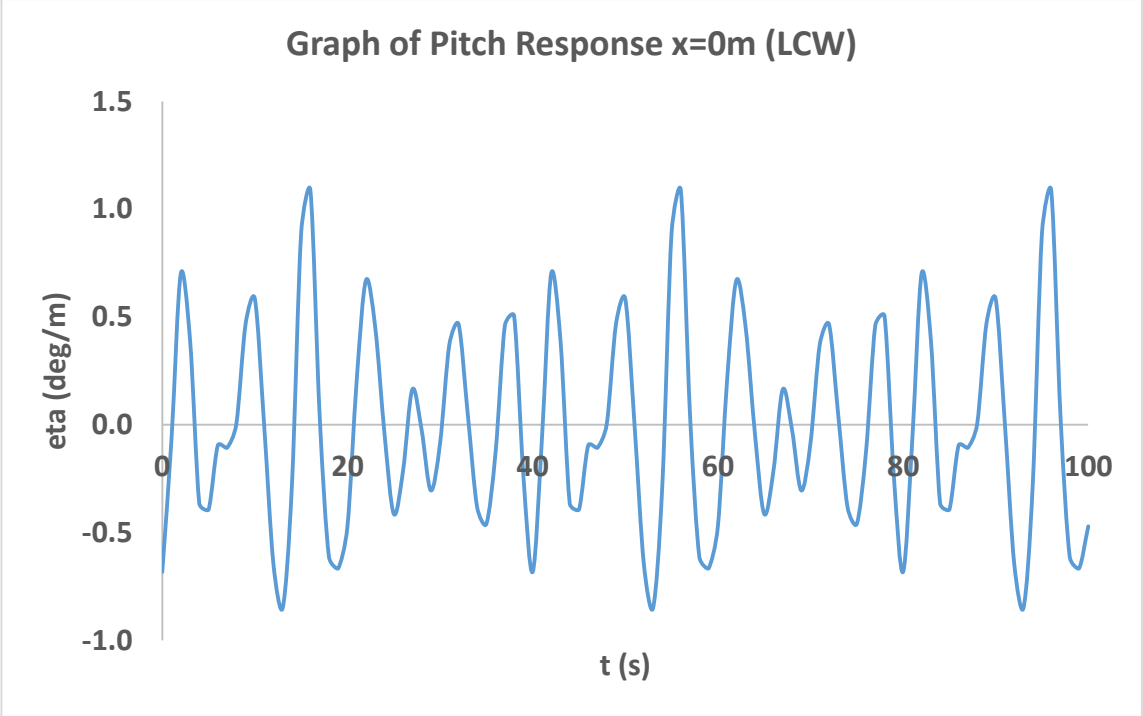

Figure 26: Response of M_y Motion for Long-Crested Waves

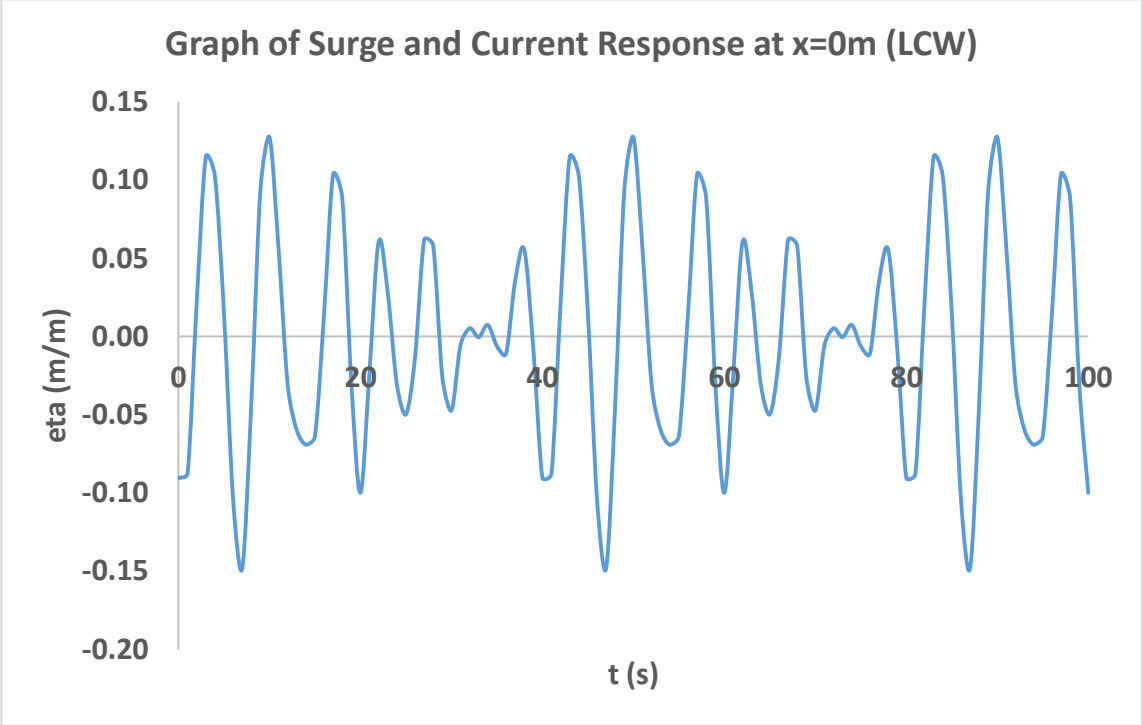

Figure 27: Response of F_x with Current Motion for Long-Crested Waves

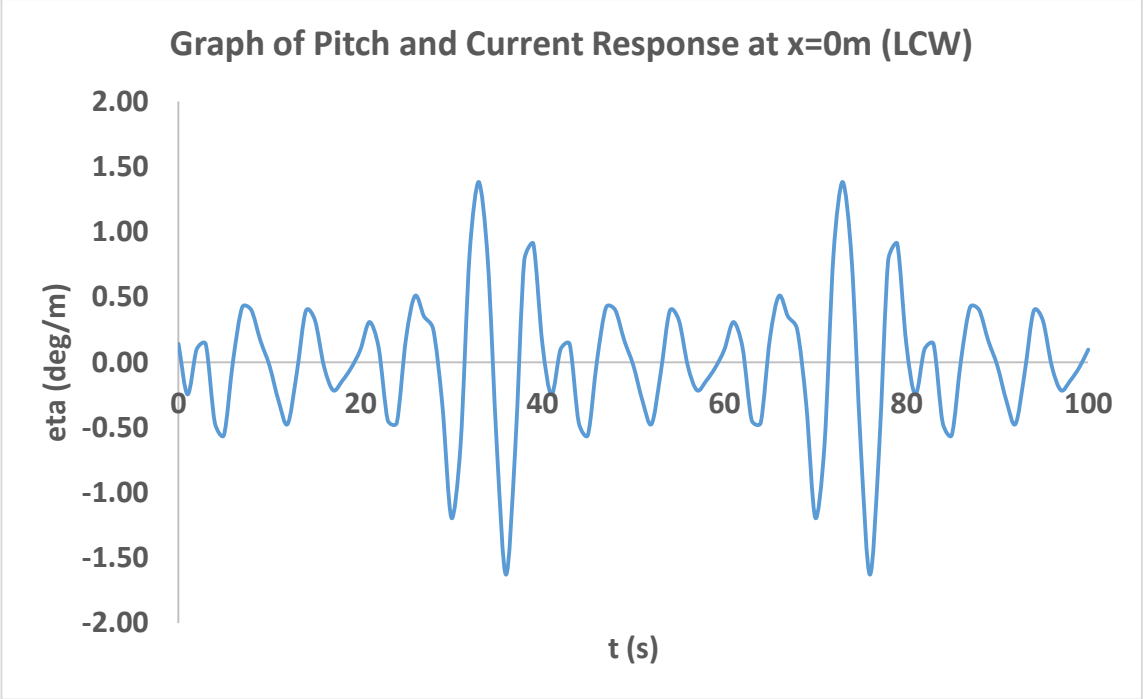

Figure 28: Response of M_y with Current Motion for Long-Crested Waves

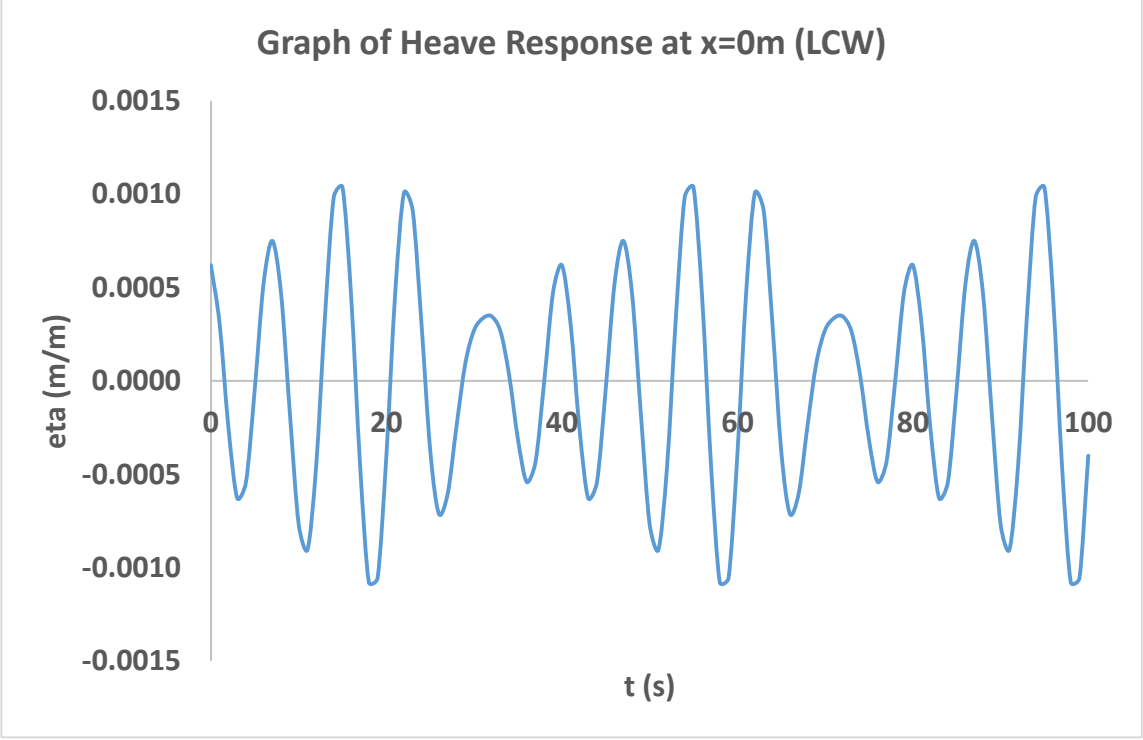

Figure 29: Response of F_z Motion for Long-Crested Waves

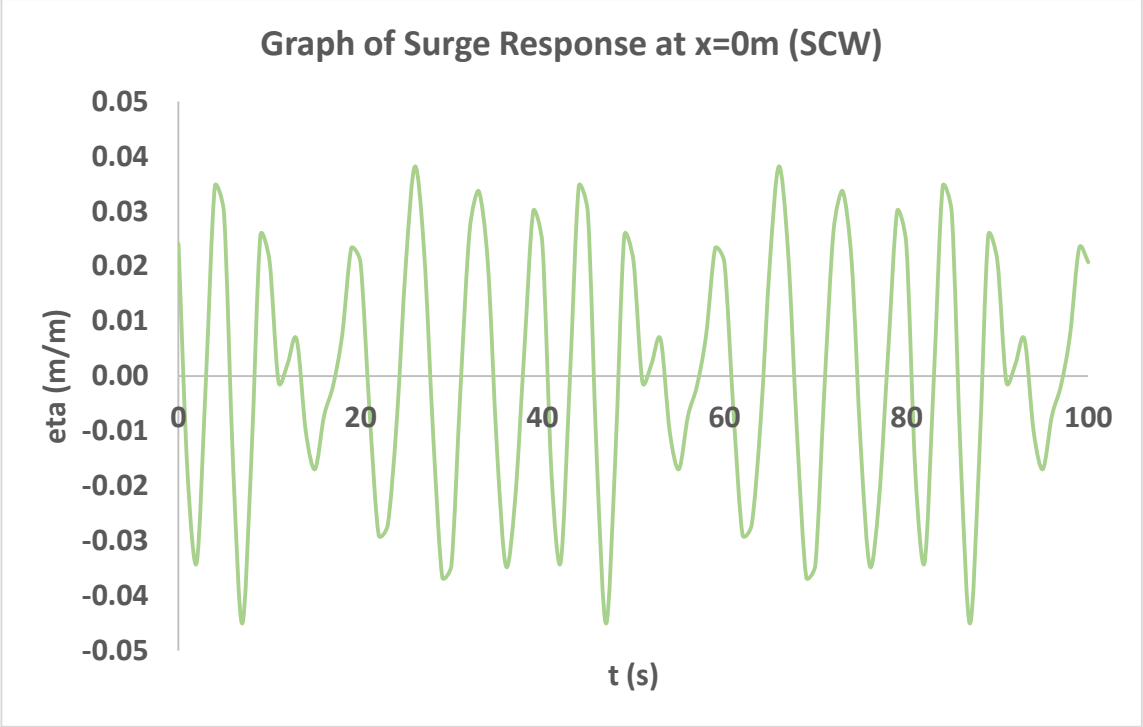

Figure 30: Response of F_x Motion for Short-Crested Waves

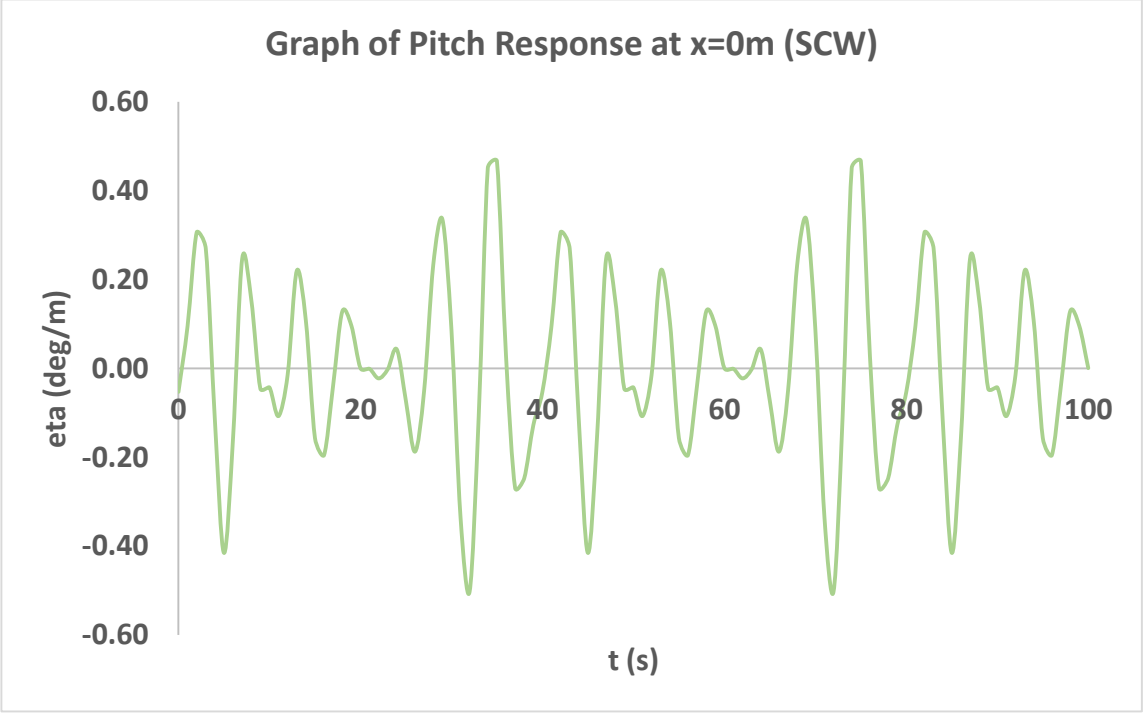

Figure 31: Response of M_y Motion for Short-Crested Waves

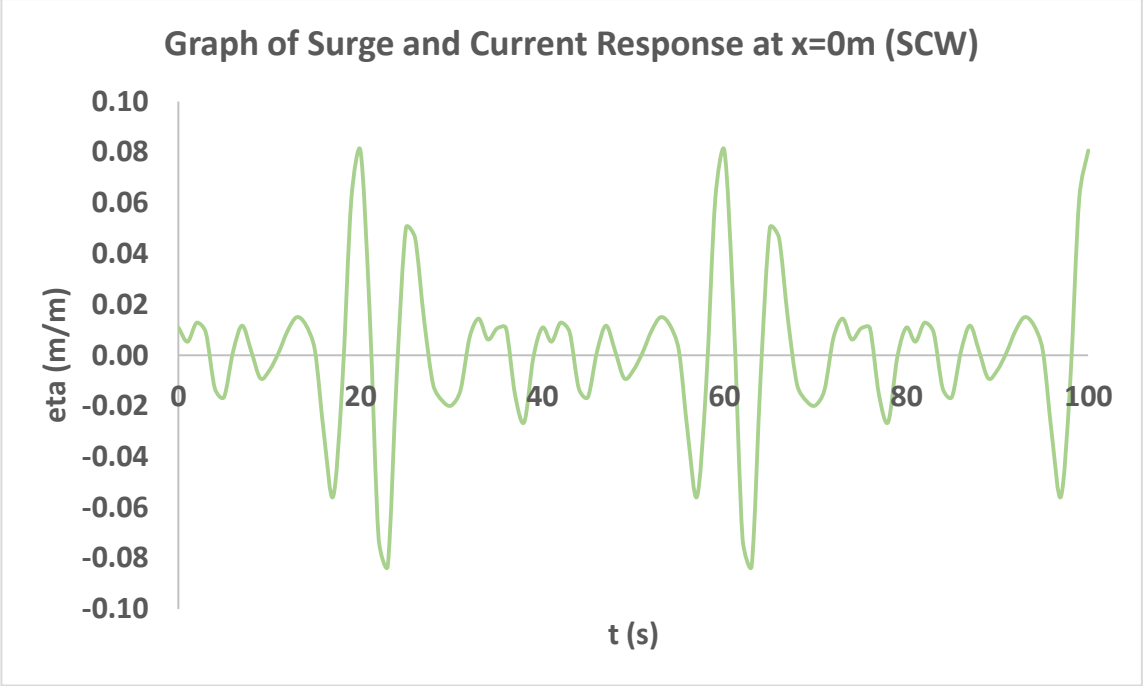

Figure 32: Response of F_x with Current Motion for Short-Crested Waves

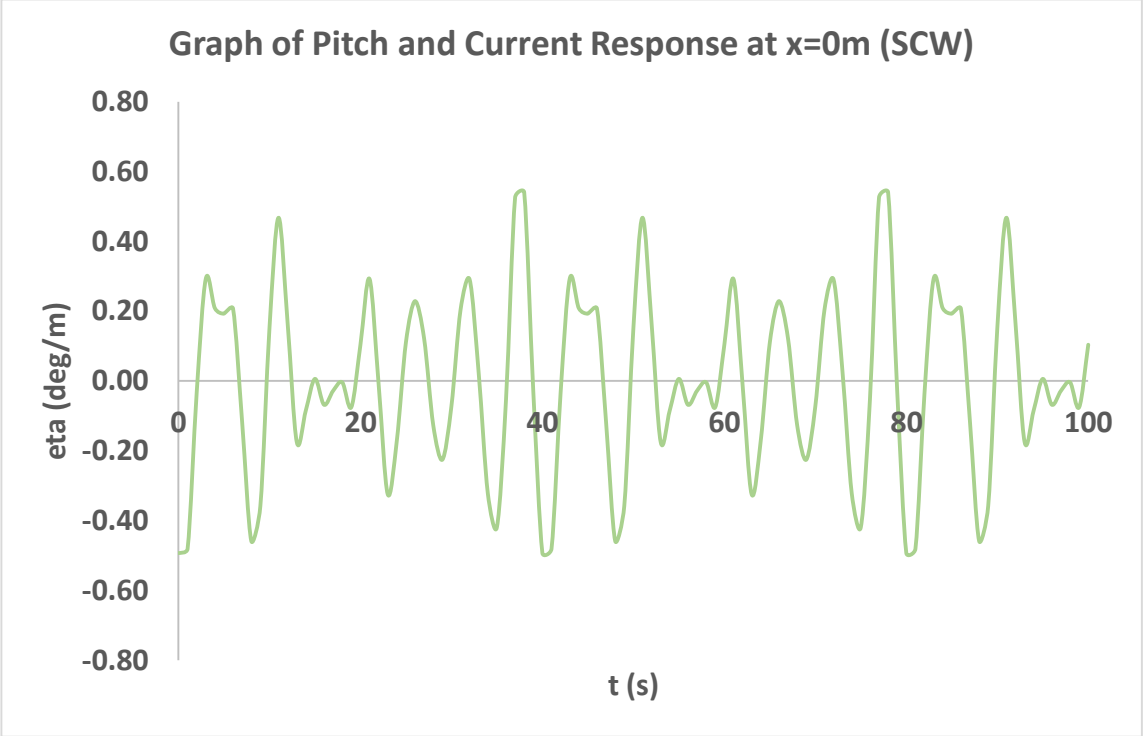

Figure 33: Response of M_y with Current Motion for Short-Crested Waves

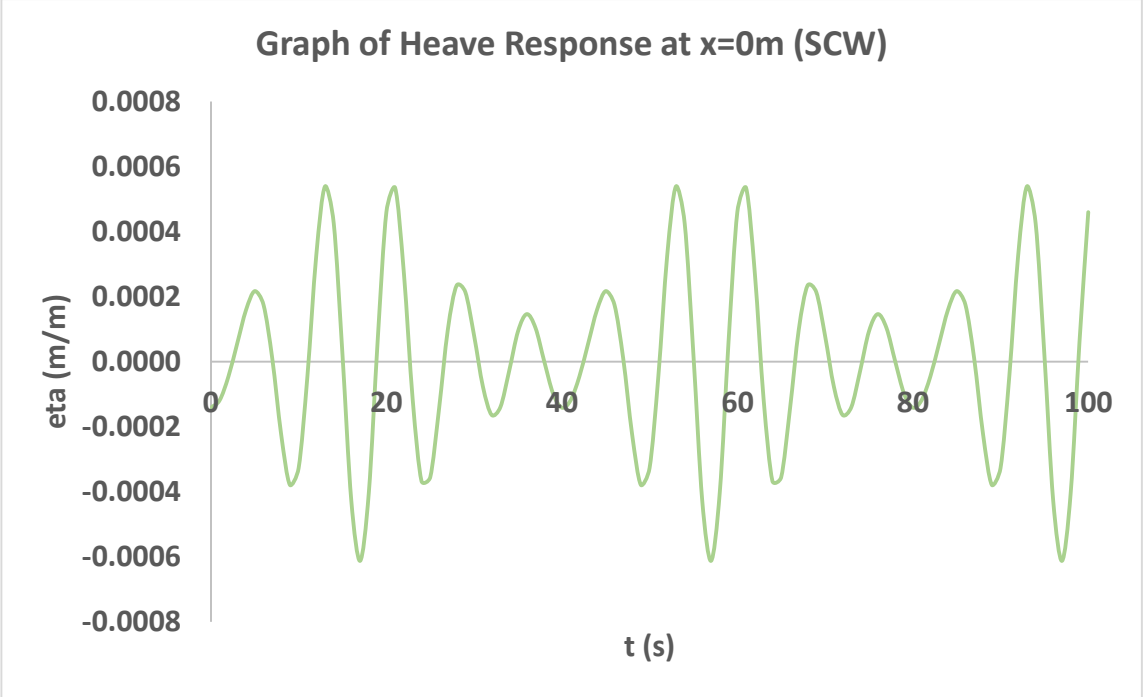

Figure 34: Response of F_z Motion for Short-Crested Waves

The dynamic responses of semi-submersible were represented by the maximum amplitude from motion response graph instead of response spectrum, $S_x(f)$ which represented for wave energy density. Thus, from the graph of motion response, the maximum amplitude of motion response for the three degrees of freedom was determined and plotted in bar chart for better illustration. According to the bar chart, it clearly showed that short-crested waves definitely gave lower dynamic responses than long-crested waves in all degrees of freedom investigated. For instance, M_y motion generated roughly 1 deg/m response under long-crested wave condition, but the response for short-crested waves was half of the value.

F_z degree of freedom produced much lower dynamic reaction as compared to F_x, which was 0.00055 m/m and 0.039226 m/m respectively in term of short-crested waves. This indicated that wave responses were substantial in F_x degree of freedom when comparing with F_z.

Besides, a summarized table was presented below including the percentage of difference between long-crested and short-crested waves for each motion. Most of the dynamic motions had percentage of discrepancy more than 50% except for M_y, which was 33.23%. This proved that the application of short-crested waves in the design of offshore structures is more optimum and economical. This result was aligned with the results from literature review, where short-crested waves have lower dynamic responses than long-crested waves.

However, for the inclusion of current into F_x and M_y motion did not affect significantly as compared to the motion without current induced (Figure 24 and Figure 25). This was because the current loading was comparatively minor in ocean than the major environmental loading, which was waves. There was an exception where for short-crested waves in surge motion, the maximum amplitude without current is approximately 50% less than the maximum amplitude with current.

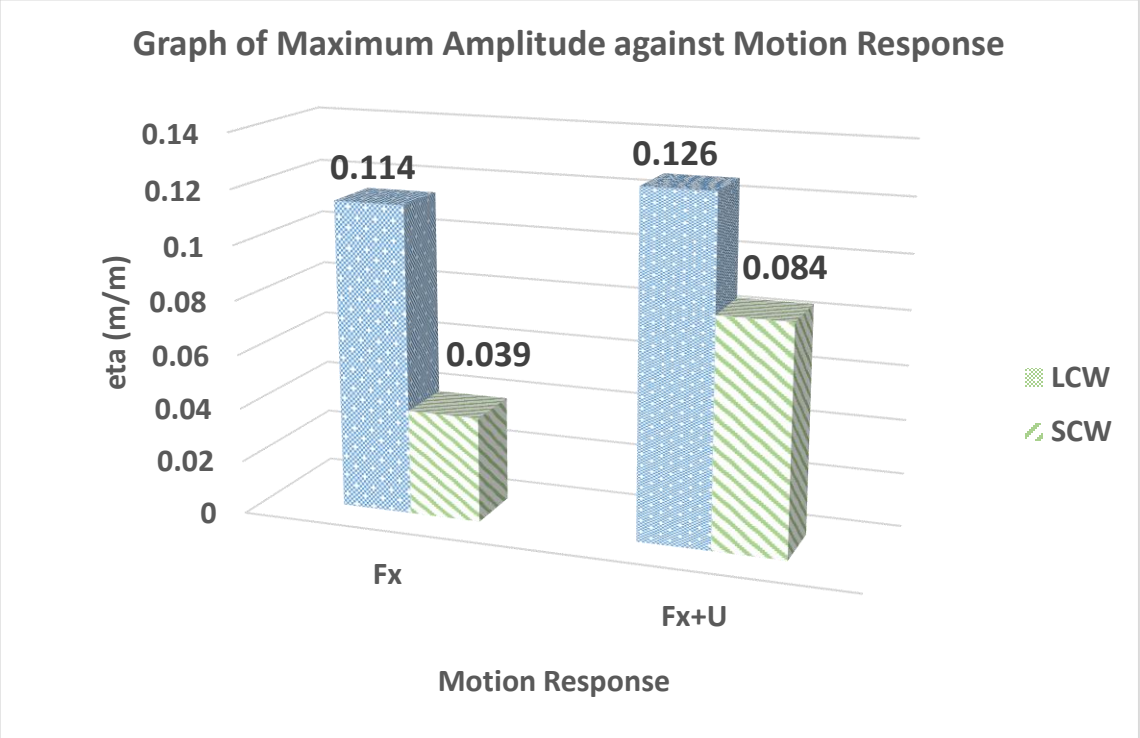

Figure 35: Comparison between F_x and F_x with Current for Long-Crested and Short-Crested Waves

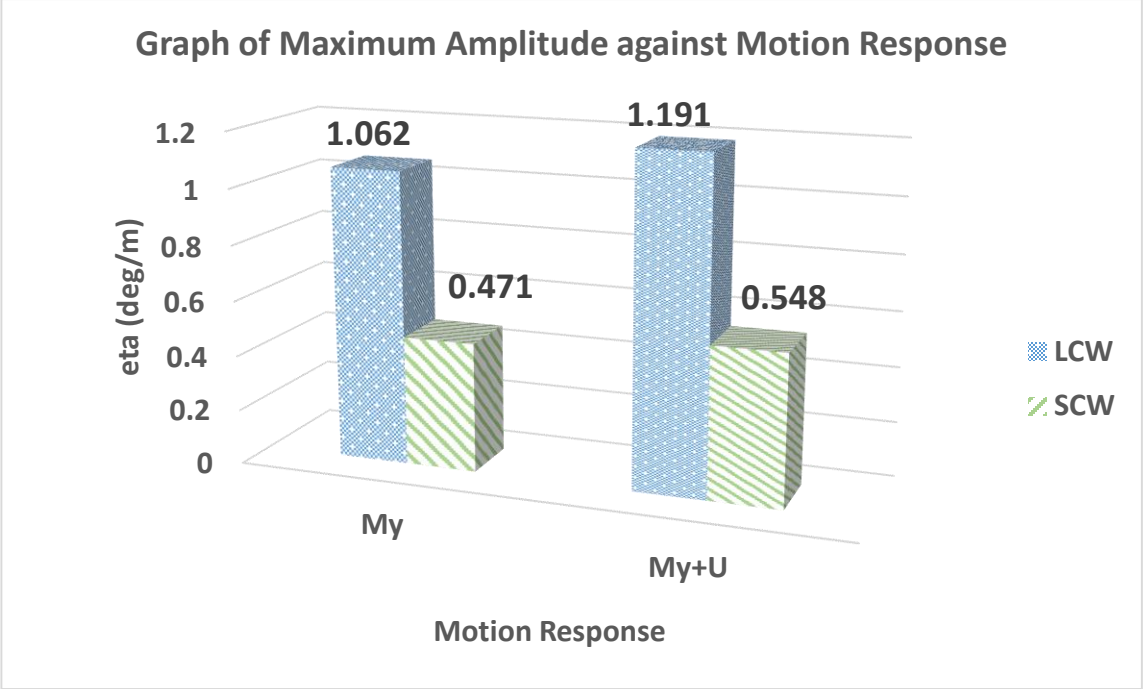

Figure 36: Comparison between M_y and M_y with Current for Long-Crested and Short-Crested Waves

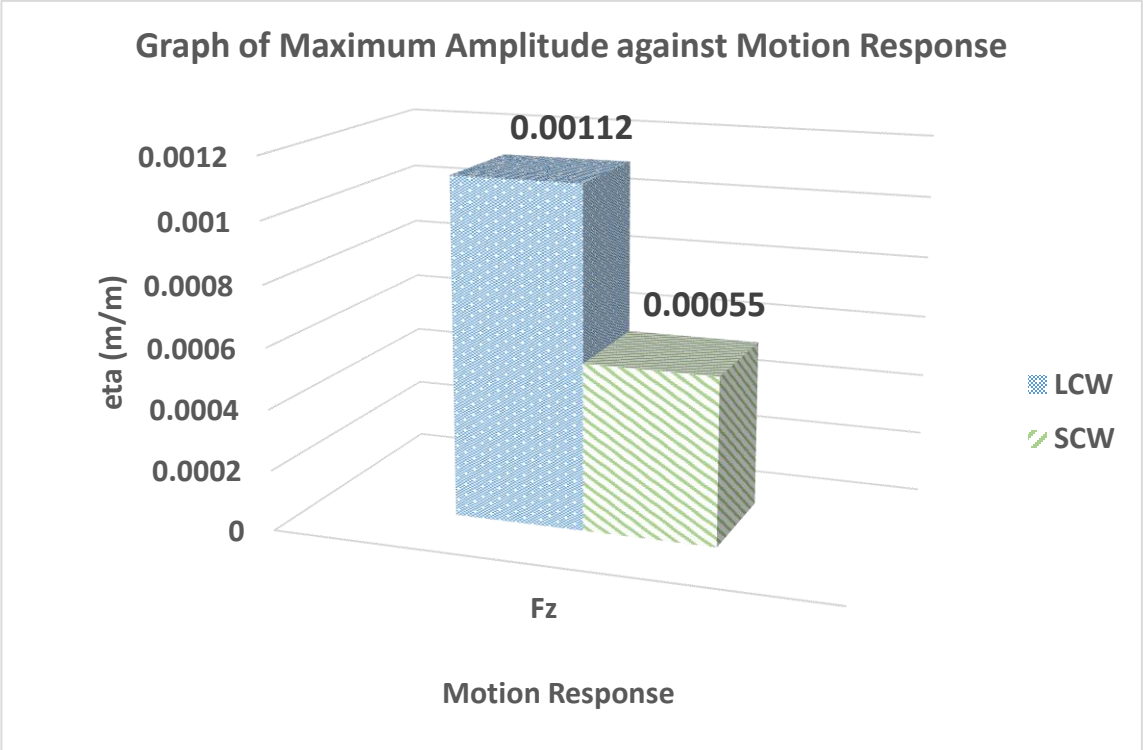

Figure 37: Comparison of F_z between Long-Crested and Short-Crested Waves

Table 4: Summary of the Maximum Amplitude of Motion Response

Maximum Amplitude	**F_x (m/m)**	**F_x+U (m/m)**	**M_y (deg/m)**	**M_y+U (deg/m)**	**F_z (m/m)**
Long-Crested Waves	0.114358	0.126407	1.02446	1.333822	0.001115
Short-Crested Waves	0.039226	0.084402	0.470709	0.547765	0.00055
Percentage of Discrepancy (%)	65.69	33.23	54.05	58.93	50.64

CHAPTER 5

CONCLUSION AND RECOMMENDATION

5.1 Conclusion

In order to obtain an optimum and economical offshore structures design, directional wave statistics could be employed rather than conventional unidirectional wave data. However, no detailed research had been performed particularly focusing on short-crested waves and current concurrently to study the dynamic responses of semi-submersible. Therefore, a numerical comparative study on a typical eight-column semi-submersible model subjected to simulated Malaysia's deep-water environmental loadings was conducted. This research was aimed to study the dynamic responses of semi-submersible model by comparing the responses subjected to long-crested and short-crested waves with current.

In the research, a frequency domain method analysis incorporated the Morison Equation was developed to compute the force components in F_x, F_z, and M_y motion. Wave spectrum from P-M model and directional wave spectrum had been computed, as well, in this study in order to obtain Response Amplitude Operator (RAO) for the structure subjected to long-crested waves, short-crested waves, and current induced at the end of the project. The RAO graph obtained in the results followed the trend, where RAO value decreased in corresponding to the increase of frequency.

The response motion spectrum was computed as well for long-crested and short-crested waves. Lastly, the results were discussed and compared by using the maximum amplitude from motion response graph to quantify the significance of short-crested waves. As the conclusion, it was summarized that the dynamic responses for short-crested waves was approximately 50% lower than long-crested waves except for M_y motion. The maximum

amplitudes obtained were 0.04 m/m, 0.47 deg/m, and 0.00055 m/m for F_x, M_y, and F_z respectively. Thus, the application of short-crested waves instead of long-crested waves is more optimum, economical, and effective in designing and costing of offshore structures.

For the inclusion of current into F_x and M_y motion, it did not affect significantly in overall as compared to the motion without current induced, where the maximum amplitudes with current loadings were 0.08 m/m and 0.55 deg/m for F_x and M_y motion respectively. Besides, it was found that the dynamic response of semi-submersible was relatively substantial at F_x motion compared to F_z motion.

In term of feasibility and relevancy, this project was feasible within time frame and scope for Final Year Project. It was also very relevant to offshore oil and gas field especially for Civil Engineering final year students. With the parallel progress to the Gantt Chart proposed, this project had been completed within time frame and the key milestones set had been achieved successfully. In conclusion, the objectives of this project had been achieved completely and successfully.

5.2 Recommendation

As reflection, there are some suggestions which will be beneficial for future learning. In future study, it is proposed that experimental study can be conducted on this relevant topic provided that the feasibility of project in term of time scale and scope can be fulfilled. With the sufficient infrastructures provided in Universiti Teknologi PETRONAS Offshore Laboratory, it is assumed that the results obtained can achieve higher accuracy and reliability. In this project, due to the constraint of time, project experiment has been substituted with numerical comparative study so that the objectives for this project can be attained within time frame.

In addition, for detailed study on this topic, different dimension of semi-submersible models can be utilized in the numerical comparative analysis with the provision of sufficient time. This can provide higher percentage of accuracy and reliability through repeating the study and interpreting the results for several times. In this project, there is only one type of semi-submersible model used in the computation due to time constraint and scope of study purposed.

Furthermore, for more thorough analysis results, it is recommended that numerical MATLAB code can be developed and applied to predict the dynamic analysis of semi-submersible due to short-crested waves. However, this definitely requires particular knowledge and skill in utilizing the software which involves complex formulation and program. As an outcome, these recommendations are anticipated to be able to further validate the results obtained and enhance the study on this topic for future learning.

REFERENCE

[1] M. Robert, "Oil and gas industry in Malaysia – An overview," in *Jurutera*, 2005, pp. 9.

[2] F. Terry, "Overview of Shell deepwater developments in Malaysia," in *Subsea Asia Conference*, 2008, pp. 9.

[3] F.Z. Sun, "Analysis of motions of semi-submersible in sea waves," in *Offshore Technology Conference*, 1980, pp. 429-442.

[4] H. Maeda, T. Ikoma, K. Masuda, C.K. Rheem, "Time domain analyses of elastic response and second order mooring force on a very large floating structure in irregular waves," *Marine Structures*, vol. 13, pp. 279-299, 2000.

[5] H.Q. Zhang, J.C. Li, "Wave loading on floating platforms by internal solitary waves," in *New Trends in Fluid Mechanics Research*, 2007, pp. 304-307.

[6] O. Yilmaz, A. Incecik, "Dynamic response of moored semi-submersible platforms to non-collinear wave, wind, and current loading," in *International Society of Offshore and Polar Engineers (ISOPE)*, 1995.

[7] A.K. Agarwal, A.K. Jain, "Dynamic behavior of offshore spar platforms under regular sea waves," in *Ocean Engineering*, vol 30, pp. 487-516, 2003.

[8] G.C. Ralls, R.L. Wiegel, "A laboratory study of short-crested wind waves," in *Corps of Engineers*, 1956.

[9] Z.B. Sun, S.X. Liu, J.X. Li, "Numerical study of multidirectional focusing wave run-up a vertical surface-piercing cylinder," in *Journal of Hydrodynamics*, vol 24, pp. 86-99, 2012.

[10] X.R. Ji, S.X. Liu, J.X. Li, W. Jia, "Experimental investigation of the interaction of multidirectional irregular waves with a large cylinder," in *Ocean Engineering*, vol 93, pp. 64-73, 2015.

[11] Y. Li, M. Lin, "Regular and irregular wave impacts on floating body," in *Ocean Engineering*, vol 42, pp. 93-101, 2012.

[12] S.P. Zhu, "Diffraction of short crested waves," *Ocean Engineering*, vol. 20. No 4, pp. 389-407, 1993.

[13] Y.J. Jian, J.M. Zhan, Q.Y. Zhu, "Short-crested wave-current forces around a large vertical circular cylinder", European Journal of Mechanics B/Fluids, vol. 27, pp. 346-360, 2008.

[14] W. Koterayama, M. Nakamura, "Drag and inertia force coefficients derived from field tests," in *Inter. J. Offshore and Polar Engineering*, 1992, pp. 161-167.

[15] P. Boccotti, F. Arena, V. Fiamma, G. Barbaro, "Field experiment on random wave forces acting on vertical cylinders," in *Probabilistic Engineering Mechanics*, vol. 28, pp. 39-51, 2012.

[16] P. Boccotti, F. Arena, V. Fiamma, A. Romolo, "Two small-scale field experiments on the effectiveness of Morison's equation," in *Ocean Engineering*, vol 57, pp. 141-149, 2013.

[17] IAHR, "Comparative analyses of multidirectional wave basin data," 1995.

[18] J.D. Fenton, "Numerical comparisons of wave analysis methods," in *Computers and Geosciences*, vol 14, No. 3, pp. 357-368, 1988.

[19] A. Hassan, M. Adi, M. Rafiqul, M. Allan, "Motion responses and incident wave forces on a moored semisubmersible in regular waves," *The International Conference on Marine Technology*.

[20] A.H. Heidari, S.M. Borghei, M. Sohrabpour, "Dynamic response of a moored semisubmersible in short-crested wave fields," *Scientia Iranica*, vol. 11, No 4, pp. 351-360, 2004.

[21] V.J. Kurian, C.Y. Ng, M.S. Liew, "Experiment investigation for the responses of semi-submersible platform subjected to bi-directional waves," in *National Postgraduate Conference*, 2011.

[22] V.J. Kurian, C.Y. Ng, M.S. Liew, "Effect of short-crested waves on the dynamic responses of truss spar platforms," in *International Society of Offshore and Polar Engineers (ISOPE)*, 2013, pp. 889-906.

[23] V.J. Kurian, C.Y. Ng, M.S. Liew, "A numerical and experimental study on motion responses of semi-submersible platforms subjected to short-crested waves," in *11th International Conference on Vibration Problems*, 2013.

[24] V.J. Kurian, C.Y. Ng, M.S. Liew, "Dynamic responses of truss spar due to wave action" *Research Journal of Applied Sciences, Engineering and Technology*, vol. 5. No 3, pp. 812-818, 2013.

[25] O.A.A. Montasir, V.J. Kurian, S.P. Narayanan, M.A.W. Mubarak, "Dynamic responses of spar subjected to waves and current" *International Conference on Construction and Building Technology*, pp. 173-182, 2008.

APPENDIX

The table below shows the RAO value obtained for each motion.

Table 5: RAO Value

Frequency (Hz)	RAO F_x (m/m)	RAO M_y (deg/m)	RAO F_x+U (m/m)	RAO M_y+U (deg/m)	RAO F_z (m/m)
0.025	0.37404213	3.829060461	1.95984076	19.97330053	2.166620676
0.050	0.292234491	2.177875318	0.641162452	4.720002107	0.176903628
0.075	0.245710058	1.811336085	0.395726568	2.859581431	0.045204165
0.100	0.192232197	1.46737918	0.279441483	2.07317317	0.01305016
0.125	0.149392019	1.209359566	0.202078529	1.573243544	0.003641419
0.150	0.119210656	1.039395003	0.154208896	1.278306234	0.000926181
0.175	0.091228397	0.862855772	0.117130121	1.04030214	0.000208594
0.200	0.064929701	0.665700428	0.086370554	0.818330515	4.09141E-05
0.225	0.054789118	0.603154104	0.070325912	0.709573825	6.9162E-06
0.250	0.039590065	0.462970009	0.052062573	0.548313988	1.00054E-06
0.275	0.034997947	0.429651129	0.045254826	0.499379629	1.23261E-07
0.300	0.027670715	0.352931537	0.036423987	0.413299553	1.28842E-08
0.325	0.023494747	0.308747856	0.030813604	0.358380882	1.13958E-09
0.350	0.01940142	0.260995501	0.025750771	0.304324901	8.51077E-11
0.375	0.015609514	0.213915017	0.021093401	0.251039064	5.35795E-12
0.400	0	0	0	0	0
0.425	0	0	0	0	0
0.450	0	0	0	0	0
0.475	0	0	0	0	0
0.500	0	0	0	0	0

The table below shows the S(f) value computed for long-crested and short-crested waves.

Table 6: S(f) Value for Long-Crested and Short-Crested Waves

Frequency (Hz)	**S(f) Long-Crested Waves m^2-sec**	**S(f) Short-Crested Waves m^2-sec**
0.000	0	0
0.025	0	0
0.050	6.44296E-68	1.36724E-68
0.075	6.32659E-12	1.34254E-12
0.100	0.005576666	0.001183405
0.125	0.753353777	0.159866637
0.150	2.633007637	0.558741574
0.175	3.078913944	0.653365831
0.200	2.476721091	0.525576539
0.225	1.746328554	0.370582429
0.250	1.182429995	0.250919438
0.275	0.79754782	0.169244904
0.300	0.543975286	0.115435141
0.325	0.377355772	0.080077382
0.350	0.266693654	0.056594151
0.375	0.19200618	0.040744977
0.400	0.140691514	0.029855667
0.425	0.104797058	0.022238626
0.450	0.079251229	0.016817633
0.475	0.06077169	0.012896153
0.500	0.047199061	0.010015952

The table below shows the $S_x(f)$ value obtained for long-crested waves.

Table 7: $S_x(f)$ Value for Long-Crested Waves

Frequency (Hz)	**$S_x(f)$ F_x m^2-sec**	**$S_x(f)$ M_y m^2-sec**	**$S_x(f)$ F_x+U m^2-sec**	**$S_x(f)$ M_y+U m^2-sec**	**$S_x(f)$ F_z m^2-sec**
0.000	0	0	0	0	0
0.025	0	0	0	0	0
0.050	5.50235E-69	3.05599E-67	2.64863E-68	1.43539E-66	2.01632E-69
0.075	3.81958E-13	2.07571E-11	9.90741E-13	5.17338E-11	1.29279E-14
0.100	0.000206076	0.012007686	0.000435468	0.023968772	9.49743E-07
0.125	0.016813331	1.101817988	0.030763753	1.864622353	9.98942E-06
0.150	0.037418147	2.844548664	0.062613932	4.302510436	2.25862E-06
0.175	0.025624632	2.292313265	0.042241053	3.332088551	1.33968E-07
0.200	0.010441524	1.097576437	0.018476024	1.658573012	4.14594E-09
0.225	0.005242212	0.635305374	0.008636876	0.879267717	8.35336E-11
0.250	0.001853309	0.253443498	0.00320499	0.355495485	1.18371E-12
0.275	0.000976881	0.147227402	0.001633377	0.198892486	1.21173E-14
0.300	0.000416505	0.067757926	0.000721696	0.092919965	9.03015E-17
0.325	0.000208302	0.035971529	0.000358291	0.048466389	4.90054E-19
0.350	0.000100388	0.018166812	0.000176845	0.024699472	1.93175E-21
0.375	4.67836E-05	0.008786133	8.54296E-05	0.012100347	5.51203E-24
0.400	0	0	0	0	0
0.425	0	0	0	0	0
0.450	0	0	0	0	0
0.475	0	0	0	0	0
0.500	0	0	0	0	0

The table below shows the $S_x(f)$ value obtained for short-crested waves.

Table 8: $S_x(f)$ Value for Short-Crested Waves

Frequency (Hz)	**$S_x(f)$ F_x m^2-sec**	**$S_x(f)$ M_y m^2-sec**	**$S_x(f)$ F_x+U m^2-sec**	**$S_x(f)$ M_y+U m^2-sec**	**$S_x(f)$ F_z m^2-sec**
0.000	0	0	0	0	0
0.025	0	0	0	0	0
0.050	1.16763E-69	6.485E-68	5.62057E-69	3.04599E-67	4.27876E-70
0.075	8.1054E-14	4.4048E-12	2.10242E-13	1.09783E-11	2.74338E-15
0.100	4.37306E-05	0.00254811	9.24092E-05	0.005086331	2.01542E-07
0.125	0.0035679	0.233813039	0.006528271	0.395685153	2.11982E-06
0.150	0.007940377	0.603631974	0.013287089	0.913021071	4.79295E-07
0.175	0.005437716	0.486443983	0.00896383	0.707091152	2.84289E-08
0.200	0.00221576	0.232912954	0.003920734	0.351960125	8.79795E-10
0.225	0.001112432	0.134815987	0.001832802	0.186586405	1.77264E-11
0.250	0.000393284	0.053782381	0.00068012	0.075438485	2.51192E-13
0.275	0.000207301	0.031242625	0.000346613	0.042206296	2.57137E-15
0.300	8.8385E-05	0.014378678	0.000153149	0.019718229	1.91626E-17
0.325	4.4203E-05	0.007633396	7.60317E-05	0.010284887	1.03993E-19
0.350	2.13029E-05	0.003855117	3.75277E-05	0.005241391	4.0993E-22
0.375	9.9278E-06	0.001864475	1.81287E-05	0.002567773	1.16969E-24
0.400	0	0	0	0	0
0.425	0	0	0	0	0
0.450	0	0	0	0	0
0.475	0	0	0	0	0
0.500	0	0	0	0	0